sp(6) ⊃ u(3) algebra of the fermion dynamical symmetry model for actinide nuclei

Sudha R. Swaminathan and K. T. Hecht
Department of Physics, The University of Michigan, Ann Arbor, Michigan 48109
(Received 23 March 1994)

The basis states generated in the sp(6) ⊃ u(3) algebra of the fermion dynamical symmetry model (FDSM) are studied. The assumption made in the FDSM that the lowest-lying states of even nuclei are states with $u = 0$ and the largest SU(3) quantum numbers is analyzed. A pairing plus quadrupole-quadrupole interaction is diagonalized for valence nucleons of the actinide region in (i) a complete basis for two protons and two neutrons, (ii) a truncated FDSM basis for 10 protons and 14 neutrons, and (iii) a strongly-coupled FDSM basis for 24 nucleons. The existence of a multiplicity of FDSM bases is taken into account. In all cases, the overlap between the truncated FDSM subspace and the full shell model space is very small for the n-identical-particle calculations. This implies that a complicated renormalization of shell model effective interactions is required before they can be used in the individual proton and neutron spaces. However, with the proper forced choice of proton and neutron bases, a strong proton-neutron quadrupole-quadrupole interaction drives the states with the largest possible FDSM-SU(3) quantum numbers to lie lowest in energy. This leads to a rotational band structure in actinide nuclei with excited rotational bands ordered by the FDSM-SU(3) quantum numbers in the strong coupling limit.

PACS number(s): 21.60.Fw, 27.90.+b

I. INTRODUCTION

The study of nuclear collective behavior in terms of the single-particle degrees of freedom of the nuclear shell model still forms one of the great challenges for our understanding of nuclear structure. Shell model dimensionalities for heavy deformed nuclei become prohibitively large even for modern computational facilities. In any case, the enormity of the bases precludes an understanding of the eigenstates in terms of the j-j coupling scheme. The pioneering work of Elliott [1,2] using group-theoretical methods, in particular the three-dimensional harmonic oscillator symmetry group SU(3), led to a physically relevant truncation scheme in light rotational nuclei whose low-lying rotational bands are dominated by a single SU(3) representation. An extension to the pseudo-SU(3) model [3] has led to an analogous truncation scheme in heavy deformed nuclei. Much of the success associated with the correspondence between the real and pseudo-oscillator shell model is related to the fact that the real quadrupole moment operator maps almost perfectly onto the corresponding pseudo-space operator of the same SU(3) symmetry [4].

The appeal of a mathematically dictated truncation of the shell model basis has led to the development of algebraic models, of which the most successful one is the interacting boson model (IBM) [5]. In the IBM, the bosonlike characteristics of nucleon pairs are exploited and the low-energy excitations of even nuclei are replaced by purely bosonic ones. The main limitation which shadows the phenomenological successes of the IBM is its nebulous connection to the many-fermion microscopic foundation of the shell model. The mapping from the shell model fermion pairs of even nuclei coupled to a total angular momentum of $J = 0$ and $J = 2$ to the s and d bosons of the IBM is very complicated. Although relatively satisfactory methods exist for the derivation of the coefficients of IBM Hamiltonians in and near the vibrational limit of the model, much less progress has been made in and near the deformed limit.

An attempt at formulating an algebraic model based on a fermion structure with only the favored S ($J = 0$) and D ($J = 2$) pairs was made by Ginocchio to gain some insights into the s, d boson pairs of the IBM [6]. In Ginocchio's model, the single-nucleon angular momenta j of the shell model are built in terms of pseudo-orbital quantum numbers k and pseudospin quantum numbers i, with $\mathbf{k} + \mathbf{i} = \mathbf{j}$. Combinations of k and i are chosen to reproduce the observed normal parity single particle j values of the major oscillator shells for nuclei with neutron and proton numbers greater than 28. For example, $k = 2$, $i = \frac{3}{2}$ gives the $s_{\frac{1}{2}}$, $d_{\frac{3}{2}}$, $d_{\frac{5}{2}}$, $g_{\frac{7}{2}}$ orbits of $N = 4$. $k = 1$, $i = \frac{1}{2}$, $\frac{7}{2}$ gives the $p_{\frac{1}{2}}$, $p_{\frac{3}{2}}$, $f_{\frac{5}{2}}$, $f_{\frac{7}{2}}$, $h_{\frac{9}{2}}$ orbits of $N = 5$. $k = 1$, $i = \frac{3}{2}$, $\frac{9}{2}$ gives the $s_{\frac{1}{2}}$, $d_{\frac{3}{2}}$, $d_{\frac{5}{2}}$, $g_{\frac{7}{2}}$, $g_{\frac{9}{2}}$, $i_{\frac{11}{2}}$ orbits of $N = 6$.

Now consider the construction of the favored S ($J = 0$) and D ($J = 2$) pairs of identical protons or neutrons. For shells with a single pseudospin $i = \frac{3}{2}$, such pairs are formed by coupling the individual k spins of the two particles to a resultant $K_p = 0$ and their i spins to $I_p = 0$, 2. These are the S and D pairs in the so-called i-active version of the model. On the other hand, for shells with a single pseudo-orbital angular momentum $k = 1$, the favored pairs of identical nucleons are obtained by coupling the two individual i spins to a resultant $I_p = 0$ and the k spins to $K_p = 0$, 2. These are the S and D pairs in the so-called k-active version of the model.

The i-active algebra is generated by the six favored pair creation operators $S^\dagger$ and $D^\dagger$, their six corresponding Hermitian conjugate pair annihilation operators, and

the sixteen one-body operators built from single-nucleon creation and annihilation operators coupled to a resultant $K_p = 0$ and $I_p = 0,\ 1,\ 2,$ and 3. These 28 k-space scalar operators generate the so(8) Lie algebra with three subalgebras; (i) so(6) + u(1), (ii) so(7), and (iii) su(2) + so(5). (We adhere to the common practice of using lower case letters for algebras and capital letters for groups).

The k-active algebra is generated by the six favored pair creation operators $S^\dagger$ and $D^\dagger$, their six corresponding Hermitian conjugate pair annihilation operators, and the nine one-body operators built from single-nucleon creation and annihilation operators coupled to a resultant $I_p = 0$ and $K_p = 0,\ 1,$ and 2. These 21 i-space scalar operators generate the sp(6) Lie algebra with a u(3) subalgebra generated by the nine one-body operators with $K_p = 0,\ 1,$ and 2. If we subtract the u(1) algebra generated by the number operator with $K_p = 0$ and $I_p = 0$ from u(3), we get the su(3) algebra. Ginocchio noted the inability to generate sufficiently large SU(3) quantum numbers and consequently sufficiently large rotational angular momenta in the k-active sp(6) algebra with the su(3) subalgebra. Due to this "fatal flaw" he abandoned this branch of his "toy" model.

The Ginocchio coupling schemes were extended to include all major shells of the shell model and reincarnated as a new model, the fermion dynamical symmetry model (FDSM) by Wu, Feng, Chen, Chen, and Guidry [7]. The high-j wrong-parity intruder orbits $h_{\frac{11}{2}}$, $i_{\frac{13}{2}}$, and $j_{\frac{15}{2}}$, which lie within the normal parity orbits of the $N = 4,\ 5,$ and 6 shells enumerated above, are assigned k spins of 0 and i spins of $i = j$ in both versions of Ginocchio's model. Pairs formed from the high-j wrong-parity intruder orbits are assumed to be coupled to angular momentum, $J = 0$. They are not expected to participate in the rotational dynamics of the nucleons at least for the rotational states below the backbending region.

The FDSM has numerous advantages. The building blocks of the model constructed from the single-fermion creation and annihilation operators reproduce the nuclear shell model completely. The fermionic structure of the pairs is very explicit. The algebraic structure of the model is amenable to the construction of symmetry-breaking operators. Since protons and neutrons are ordered into their respective shells separately, n identical particle calculations can be performed which preserve the individual nucleon degrees of freedom. The protons and neutrons can then be coupled together within a chosen algebraic framework of the model. The validity of the FDSM as a phenomenological model has also been established by the existence of effective interactions in the model space which reproduce the observed physical phenomena associated with the symmetry limits of the appropriate group chains.

The FDSM basis states are described in terms of the generalized seniority quantum number u, which is defined as the number of nucleons that do not couple to form the favored S, D pairs. The lowest energy states in the FDSM are built entirely from the favored S, D pairs. In even nuclei, for example, these are purely states with $u = 0$. Then a state with one pair of identical nucleons whose K_p and I_p spins for either the so(8) or sp(6) algebras are not the favored combinations is built. This is the state with generalized seniority $u = 2$. States with more than two particles and with generalized seniority $u = 2$ can be constructed by coupling the necessary number of favored S, D pairs to the state with $u = 2$. The states with generalized seniority $u = 2, u = 4, \ldots$ are assumed to lie at a higher energy than the $u = 0$ states which constitute the model space. In actual applications of the FDSM, this truncation from the shell model space to the $u = 0$ subspace is effected by model Hamiltonians built entirely from group generators which cannot mix states of different u. In the decoupled FDSM subspace the lowest eigenstates of even nuclei are thus assumed to be pure $u = 0$ states. Appreciable admixtures of states with $u \geq 2$ in complete shell model calculations would question the validity of this fundamental assumption of the FDSM.

The FDSM has in fact been criticized by Halse because the exact eigenstates of realistic shell model Hamiltonians in the *sd* shell have very little overlap with the pure $u = 0$ states of the FDSM [8] and because the favored D pairs of the FDSM are very different from D pairs derived from Hartree-Fock-Bogoliubov and other realistic calculations [9] in ^{156}Gd. Although the *necessity* of a strong overlap between "realistic" shell model eigenstates and the highly truncated $u = 0$ states of the FDSM has been questioned [10], a further test of the microscopic validity of the model is strongly indicated [11].

Our reason for choosing the Sp(6) $\supset$ U(3) group chain for this study is twofold. The first is to establish whether the presence of the SU(3) symmetry automatically leads to rotational spectra. The second reason is a mathematical one. If the n-particle basis states are labeled with SU(3) quantum numbers, then the operator matrix elements can be given as explicit functions of SU(3) coefficients. This is a significant advantage since there is an extensive SU(3) code from which the necessary Racah, generalized Wigner and 9j-type coefficients are easily obtained [12]. On the other hand, such tools for detailed calculations are not available for the so(8) subalgebras, namely, so(7), so(6), and so(5).

The motivation for studying the actinide nuclei is also twofold. The mathematical one stems from the presence of the Sp(6) $\supset$ U(3) group chain for both protons and neutrons. In actinide nuclei, protons fill the $N = 5$ shell while neutrons fill the $N = 6$ shell. Thus both are classified with $k = 1$ in the k-active Sp(6) $\supset$ U(3) branch of the FDSM with readily available SU(3) technology. In addition, actinide nuclei with many active protons and neutrons exhibit beautifully rotational spectra. The goodness of Elliott's SU(3) symmetry is based on the dominance of a strong quadrupole-quadrupole $(Q \cdot Q)$ interaction which automatically leads to the observation of low-lying rotational spectra [13]. The SU(3) symmetry in the FDSM is, however, quite different from Elliott's SU(3) symmetry and its pseudo-SU(3) analogue. Will the SU(3) symmetry in the FDSM also lead to rotational spectra? The results presented in Secs. VI and VII address this question and assess the rotational nature of the SU(3) symmetry imposed on both the protons and neutrons of the actinide nuclei through the FDSM classification.

Since actinide nuclei exhibit beautifully rotational spectra, this leads us to first reexamine Ginocchio's "fatal flaw." The sp(6) ⊃ u(3) algebra was discarded by Ginocchio because the limit on the SU(3) quantum numbers $(\lambda\mu)$ and consequently on the value of the total angular momentum J for n particles failed to produce the maximum value of J observed in the rotational bands of ^{20}Ne and ^{24}Mg. For the actinides, the limit on J is $J = 24$ when ten protons with $(\lambda\mu) = (10\ 0)$ are coupled to fourteen neutrons with $(\lambda\mu) = (14\ 0)$ to give $(\lambda\mu) = (24\ 0)$. The observed rotational spectra in the actinide nuclei reach J values of $\approx 30 - 40$ before backbending signals the possible participation of wrong-parity intruder levels. Higher values of the total angular momentum in the needed J range can, however, be obtained within the framework of the FDSM, if single-particle states of the $N = 7$ shell with $j = \frac{11}{2}$, $\frac{13}{2}$, and $\frac{15}{2}$ are admixed into the proton orbits of the $N = 5$ shell. The Nilsson model gives considerable justification for this, since the downward sloping Nilsson orbits particularly from the $j_{\frac{15}{2}}$ and $h_{\frac{11}{2}}$ members of the $N = 7$ shell reach to the middle of the $N = 5$ levels in strongly deformed prolate nuclei. The single-particle states $j = \frac{11}{2}$, $\frac{13}{2}$, and $\frac{15}{2}$ can be obtained in the k-active scheme of the FDSM with $k = 1$ and $i = \frac{13}{2}$. The highest value of $(\lambda\mu)$ which can be obtained for the protons is now equal to $(24\ 0)$. The coupling of $(\lambda\mu) = (24\ 0)$ for the protons with a $(\lambda\mu) = (14\ 0)$ for the neutrons results in a $(\lambda\mu)$ of $(38\ 0)$ and a maximum J value of 38. The allowed SU(3) states with quantum numbers $(\lambda\mu)$ which are used in labeling the initial and final states in our calculations are given in Ref. [14] for the $N = 5$ shell, in Sec. III for the $N = 6$ shell, and in Ref. [15] for the mixed $N = 5, 7$ shells. Even higher J values could in principle be obtained if single-particle states from the $N = 8$ shell were to be admixed into the neutron orbits of the $N = 6$ shell.

The group generators which make up the FDSM Hamiltonians are built from the single-nucleon creation and annihilation operators of the shell model basis $a^\dagger_{jm}, a_{jm}$ which are first expressed in terms of the $b^\dagger, b$ operators of the FDSM basis as follows:

$$a^\dagger_{jm} = \sum_{m_k m_i} \langle k m_k i m_i | j m \rangle b^\dagger_{k m_k i m_i}, \tag{1}$$

$$a_{jm} = \sum_{m_k m_i} \langle k m_k i m_i | j m \rangle b_{k m_k i m_i}. \tag{2}$$

Furthermore,

$$\tilde{b}_{k m_k i m_i} \equiv (-1)^{k - m_k + i - m_i} b_{k - m_k i - m_i}. \tag{3}$$

For actinide nuclei classified in the k-active scheme with the total i-space spins I_p, M_{I_p} equal to 0, there is only one $S^\dagger$ pair with K_p, M_{K_p} also equal to 0 as given in Eq. (4). The five $D^\dagger$ pairs with $K_p = 2$ and $\mu = 2, 1, 0, -1, 2$ are given by Eq. (5) and the nine operators P^r_μ, with $r = 0, 1, 2$ which generate the u(3) ≡ su(3) × u(1) algebra are given as Eq. (6). The four quantum numbers outside the square bracket in Eqs. (4)–(6) refer to the total spins $K_p, M_{K_p} = \mu$, I_p, M_{I_p} obtained by coupling the k and i spins for each particle. The SU(3) tensor character of the operators is discussed later when they are generalized as the $A^\dagger$ and P operators in the vector coherent state (VCS) method:

$$S^{\dagger 0}_0 = \sum_i \frac{1}{2}\sqrt{3(2i+1)}[b^\dagger_{ki} \times b^\dagger_{ki}]_{0000}, \tag{4}$$

$$D^{\dagger 2}_\mu = \sum_i \frac{1}{2}\sqrt{3(2i+1)}[b^\dagger_{ki} \times b^\dagger_{ki}]_{2\mu 00}, \tag{5}$$

and

$$P^r_\mu = \sum_i \frac{1}{2}\sqrt{3(2i+1)}[b^\dagger_{ki} \times \tilde{b}_{ki}]_{r\mu 00}. \tag{6}$$

To test the assumptions of the model, more realistic Hamiltonians constructed from microscopically based operators must be used to examine the generalized seniority composition of the lowest eigenstates. Since the simple algebraic framework of the FDSM makes it possible to construct such operators, it is reasonable to require that such a test of the model be performed. The difficulty in deriving matrix elements of operators that are not generators of the relevant group algebras has prevented such tests of the FDSM until recently. Since the quadrupole moment operator plays a central role in driving nuclei to deformed shapes leading to low-lying rotational spectra, a semirealistic interaction for the actinide nuclei should include a $Q \cdot Q$ interaction built from the real quadrupole moment operator Q. The effective interactions used in this investigation are therefore chosen to be simple $J = 0$ pairing plus $Q \cdot Q$ interactions or FDSM pairing plus $Q \cdot Q$ interactions. The techniques used to calculate the matrix elements of such operators are described in Sec. II.

The construction of the favored D pair in the FDSM does not depend on the relative phases of the radial wave functions of the harmonic oscillator shell model with different values of orbital angular momentum l. The matrix elements of physically relevant operators, such as the ones that make up the Hamiltonian, must be independent of such phase choices. However, the overlap of the low-lying two-particle shell model energy eigenstates with the FDSM two-particle states having generalized seniority $u = 0$ may be larger or smaller for certain phase choices. Effectively, this results in several FDSM bases: two for the $N = 5$ and four for the $N = 6$ shell. The coefficients of Q transformed to these FDSM bases are tabulated in Sec. IV, which also includes a description of a rigorous check of our calculations using the pseudo-SU(3) model.

Three types of calculations have been performed using the formulas from Sec. II, the relevant SU(3) states from Sec. III, and the Q coefficients from Sec. IV. The calculations are described along with their results in Secs. V–VII.

First, a complete calculation has been performed for two valence protons and two valence neutrons of the actinide region. No truncation of the shell model space is

necessary for this calculation. A Hamiltonian consisting of an FDSM pairing term and a $Q\cdot Q$ term is diagonalized in the two-particle basis and the resulting eigenstates are analyzed. The calculation is described in detail in Sec. V and the contribution of the states with $u = 0$ to the lowest eigenstates of total angular momentum $J = 0, 2$ is given. The results are presented for the two independent FDSM bases for the protons and the four independent FDSM bases for the neutrons.

The second complete calculation is a diagonalization of a $J = 0$ pairing plus $Q \cdot Q$ interaction in the pure $u = 0$ space, separately for ten valence protons and fourteen valence neutrons of the actinide region. These nucleon numbers have been chosen so that the possible SU(3) quantum numbers $(\lambda\mu)$ can range from very low values such as (02) or (20) to the highest possible permitted by the Pauli principle in the $N = 5$ and $N = 6$ shells, i.e., (10 0) for the protons and (14 0) for the neutrons. The purpose here is to examine the nature of the FDSM-SU(3) symmetry. In Elliott's SU(3) symmetry, an attractive, real $Q \cdot Q$ interaction drives the lowest eigenstates to be dominated by the highest possible SU(3) quantum numbers and leads to rotational spectra. As shown in Sec. VI, this test is not met by the FDSM-SU(3) symmetry. In the separate proton space, the (10 0) symmetry is far from dominant in the lowest eigenstates. Similarly, the separate neutron space calculation leads to low-lying eigenstates with only very small percentages of (14 0).

The third calculation, presented in Sec. VII, assesses the effect of a strong coupling of proton and neutron configurations via a proton-neutron $Q \cdot Q$ interaction. For this purpose, the ten protons are forced to be in the (10 0) symmetry and the fourteen neutrons in the (14 0) symmetry, effectively making them the dominant $u = 0$ representations, contrary to the results of Sec. VI. Then a $J = 0$ pairing plus $Q \cdot Q$ interaction is diagonalized in the strongly coupled proton-neutron basis. Now, we find that, with the proper phase choices the lowest eigenstates are dominated by the highest possible SU(3) representation in the coupled basis with $(\lambda\mu) = (24\ 0)$, and the low-energy spectra contain the rotational bands expected from the first few highest SU(3) representations.

These somewhat contradictory results are summarized and discussed in Sec. VIII.

II. MATRIX ELEMENTS IN THE Sp(6) ⊃ U(3) SCHEME

The analytical expressions for the matrix elements of the most general operators in the sp(6) ⊃ u(3) algebra of the FDSM have been derived by vector coherent state (VCS) theory [16]. An outline of the strategy for deriving the expressions which were used in our calculations, is given below, along with definitions of the symbols.

The state vectors we are interested in consist of an $(n_1 + n_2 + n_3)$-degree polynomial of $S^\dagger, D^\dagger$ coupled to the generalized seniority $u = \sigma_1 + \sigma_2 + \sigma_3$ particle state. Standard angular brackets $|\ \rangle$ are used to denote the state vectors of the coupled basis in ordinary Hilbert space. With $A^\dagger = S^\dagger, D^\dagger$,

$$[Z^{[n_1n_2n_3]}(A^\dagger) \times |[\sigma_1\sigma_2\sigma_3]\rangle]^{[\omega_1\omega_2\omega_3]\rho}_{\alpha} \equiv |[[n] \times [\sigma]][\omega]\rho;\alpha\rangle \equiv |\phi_{[n]\rho}\rangle. \quad (7)$$

The U(3) irreducible representation (irrep) which is labeled as $[n] \equiv [n_1n_2n_3]$ gives the collective quantum numbers for the favored S, D pair subspace whereas the one labeled as $[\sigma] \equiv [\sigma_1\sigma_2\sigma_3]$ gives the intrinsic quantum numbers of the u nucleons that do not couple to form the S, D pair subspace. The intrinsic and collective irreducible representations couple to form the U(3) irrep $[\omega] \equiv [\omega_1\omega_2\omega_3]$. The coupling of $[\sigma]$ and $[n]$ can give a particular $[\omega]$ more than once. This multiplicity is denoted by the label ρ. The U(3) subgroup labels including K, M_K are denoted by the label α.

The state vectors of Eq. (7) are difficult to normalize and do not form an orthonormal set. The overlap is given in terms of a Hermitian matrix $(KK^\dagger)$ as

$$\langle\phi_{[n']\rho'}|\phi_{[n]\rho}\rangle = KK^\dagger_{[n']\rho',[n]\rho}. \quad (8)$$

An orthonormal set of state vectors is obtained by a mapping to the Bargmann z space. These state vectors are specified by polynomials of z-space functions with even values for n_1, n_2 and n_3; and round brackets $(\ )$ are used to denote them:

$$[Z^{[n_1n_2n_3]}(z) \times |[\sigma_1\sigma_2\sigma_3]\rangle]^{[\omega_1\omega_2\omega_3]\rho}_{\alpha} \equiv |\,[[n] \times [\sigma]]\,[\omega]\rho;\alpha) \equiv |\phi_{[n]\rho}). \quad (9)$$

The overlap for the state vectors of Eq. (9) is given as

$$(\phi_{[n']\rho'}|\phi_{[n]\rho}) = \delta_{[n][n']}\delta_{\rho\rho'}. \quad (10)$$

The operators O which act on the state vectors are also transformed into the Bargmann z space. These z-space realizations $\Gamma(O)$ exist for both the collective operators, $Z^{[n_1n_2n_3]}(z)$ as well as the intrinsic operators such as the single-fermion operators $b^\dagger, b$, the pair-creation and pair-annihilation operators, and the one-body operator. The collective and intrinsic operators commute with each other. The VCS realization of state vectors and operators ensures that the intrinsic part of the operator acts only in the subspace of u particles and the collective part acts only in the S, D pair subspace.

The z-space realization $\Gamma(O)$ of an operator O is a nonunitary realization. The unitary realization $\gamma(O)$ is defined by taking an operator realization of the matrix K as follows:

$$\gamma(O) = K^{-1}\Gamma(O)K. \quad (11)$$

The K and K^{-1} matrices can be explicitly written in terms of the unitary matrix U, which is used to diagonalize the $KK^\dagger$ matrix and the nonzero eigenvalues, λ_ν, of this matrix:

$$(K)_{[n]\rho,\nu} = (U^\dagger)_{[n]\rho,\nu}\sqrt{\lambda_\nu}. \quad (12)$$

$$(K^{-1})_{\nu,[n]\rho} = \frac{1}{\sqrt{\lambda_\nu}}\,U_{\nu,[n]\rho}. \quad (13)$$

In the sp(6) ⊃ u(3) algebra generated in the k-active

scheme of the FDSM with $k = 1$, the single-fermion-creation operator $b^\dagger$ is a U(3) tensor with the U(3) irrep $[\omega] \equiv [1]$, and the single-fermion-annihilation operator $\tilde{b}$ is a U(3) tensor with the U(3) irrep $[\tilde{\omega}] \equiv [11]$. Both operators are actually double tensors with SU(3) symmetry in k space and SU(2) symmety in i space. The k- and i-space quantum numbers are $\alpha \equiv K, M_K$ and I, M_I respectively. The conjugation rules for the $b^\dagger, \tilde{b}$ operators are given by

$$(T^{(\omega)I}_{\alpha M_I})^\dagger = T^{(\tilde{\omega})I}_{\tilde{\alpha}-M_I}(-1)^{\chi(\omega,\alpha)}(-1)^{I-M_I}, \tag{14}$$

where $(w) \equiv (\lambda_\omega \mu_\omega) \equiv (\omega_1 - \omega_2, \omega_2 - \omega_3)$, $(\tilde{\omega}) \equiv (\mu_\omega \lambda_\omega)$, and $\tilde{\alpha} \equiv K, -M_K$. The phase factor $\chi(\omega, \alpha)$ is the SU(3) analog of the well-known angular momentum-conjugation phase factor $(-1)^{I-M_I}$. Since it is somewhat dependent on phase conventions and the choice of the quantum number α, it is not specifically defined. It does not appear in the final form of the reduced matrix elements although it is used in their derivation.

The pair and one-body operators used in our calculations are given below

$$A^\dagger(ii')^{(\omega_p)}_{K_p M_{K_p} I_p M_{I_p}} = [b^\dagger_{ki} \times b^\dagger_{ki'}]^{(\omega_p)}_{K_p M_{K_p} I_p M_{I_p}}, \tag{15}$$

$$A(ii')^{(\tilde{\omega}_p)}_{K_p M_{K_p} I_p M_{I_p}} = [\tilde{b}_{ki} \times \tilde{b}_{ki'}]^{(\tilde{\omega}_p)}_{K_p M_{K_p} I_p M_{I_p}}, \tag{16}$$

$$P(ii')^{(p)(\omega_o)}_{K_p M_{K_p} I_p M_{I_p}} = \frac{1}{2}[b^\dagger_{ki} \times \tilde{b}_{ki'}]^{(\omega_o)}_{K_p M_{K_p} I_p M_{I_p}} \tag{17}$$

$$\mp(-1)^{i+i'-I_p}\frac{1}{2}[b^\dagger_{ki'} \times \tilde{b}_{ki}]^{(\omega_o)}_{K_p M_{K_p} I_p M_{I_p}}. \tag{18}$$

These expressions are taken from Ref. [16] and differ from Eqs. (4)–(6) by the FDSM normalization factor $\frac{1}{2}\sqrt{(2k+1)(2i+1)}$ for $k = 1$. The SU(3) tensor character of the operators is also included here in the form of the SU(3) irreps (ω_p), $(\tilde{\omega}_p)$, and (ω_o). These are obtained by coupling the SU(3) irreps for the single-fermion operators as follows; (10) and (10) couple to give (ω_p) equal to (20) or (01), (01) and (01) couple to give $(\tilde{\omega}_p)$ equal to (02) or (10), and (10) and (01) couple to give (ω_o) equal to (11) or (00). The individual k, i, m_k, and m_i values couple to K_p, I_p, M_{K_p}, and M_{I_p}, respectively. Furthermore, a specific phase dependence is introduced in the one-body operator of Eq. (18) for $i \neq i'$ whose effect on the n-particle calculations will be discussed in the later sections. The upper sign $(-)$ gives symmetry in k space. In this case, the symbol (p) becomes (s) and (ω_o) = (11) or (00). The lower sign $(+)$ gives antisymmetry in k space. Now, the symbol (p) becomes (a), and (ω_o) = (11).

We aim to construct the matrix element of an arbitrary tensor operator O, in an orthonormal basis of the Hilbert space $|[[n] \times [\sigma]][\omega]\rho; \alpha\rangle$. We first write down the matrix element of the unitary realization of the operator $\gamma(O)$ in an orthonormal basis of z space $|[[n] \times [\sigma]][\omega]\rho; \alpha)$. Then we use the K and K^{-1} matrices to transform it into the matrix element of the nonunitary realization of the operator $\Gamma(O)$ in the orthonormal basis of z space. This procedure is explicitly written down in terms of the reduced matrix elements as follows:

$$\begin{aligned}\langle[[n'] \times [\sigma']][\omega']\nu';\ I'\|O^{[\omega_o]I_p}\|[[n] \times [\sigma]][\omega]\nu;\ I\rangle_{\rho_o} &= ([[n'] \times [\sigma']][\omega']\nu';\ I'\|\gamma(O)^{[\omega_o]I_p}\|[[n] \times [\sigma]][\omega]\nu;\ I)_{\rho_o} \\ &= \sum_{[n]\rho}\sum_{[n']\rho'}\{K^{-1}([\sigma'][\omega'])_{\nu',[n']\rho'}K([\sigma][\omega])_{[n]\rho,\nu} \\ &\quad \times ([[n'] \times [\sigma']][\omega']\rho';\ I'\|\Gamma(O)^{[\omega_o]I_p}\|[[n] \times [\sigma]][\omega]\rho;\ I)_{\rho_o}\}. \end{aligned} \tag{19}$$

The triple-barred matrix element of Eq. (19) is reduced in the SU(3) symmetry of k space as well as in the SU(2) symmetry of i space. The label ρ_o is the multiplicity in the coupling of $[\omega]$ and $[\omega_o]$ to $[\omega']$.

Let

$$M \equiv ([[n'] \times [\sigma']][\omega']\rho'; I'\|\Gamma(O)^{[\omega_o]I_p}\|[[n] \times [\sigma]][\omega]\rho;\ I)_{\rho_o}. \tag{20}$$

The reduced matrix elements M of the one-body operators $P(ii')$ of Eq. (18) are illustrated below for the simplest case with $u' = u - 2$.

$$M = (-1)^{\hat{\omega}_p} c^{(p)}_{(\omega_o)} \begin{bmatrix} [\sigma] & [n] & [\omega] & \rho \\ [\tilde{\omega}_p] & [2] & [\omega_o] & - \\ [\sigma'] & [n'] & [\omega'] & \rho' \\ - & - & \rho_o & \end{bmatrix} \times ([n']\|z\|[n])\langle[\sigma'];\ I'\|\|A(ii')^{(\tilde{\omega}_p)}_{I_p}\|\|[\sigma];\ I\rangle, \tag{21}$$

with

$$\langle[\sigma'];\ I'\|\|A(ii')^{[\tilde{\omega}_p]}_{I_p}\|\|[\sigma];\ I\rangle = \sum_{[\sigma'']}\sum_{I''}\{U([\sigma][11][\sigma'][11];\ [\sigma''][\tilde{\omega}_p])U(Ii'I'i;\ I''I_p)(-1)^{i+i'-I_p+\hat{\omega}_p} \times\langle[\sigma'];\ I'\|\|\tilde{b}^{[11]}_i\|\|[\sigma''];\ I''\rangle\langle[\sigma''];\ I''\|\|\tilde{b}^{[11]}_{i'}\|\|[\sigma];\ I\rangle\}. \tag{22}$$

The slightly more complicated case for $u' = u$ can be taken from Table IV of Ref. [16]. Equations (21) and (22) are given here partly to illustrate the general complexity of the expressions and partly to correct an error of Ref. [16]. In the $9(\lambda\mu)$ coefficient of Eq. (21), the irrep [2] replaces the irrep $[\omega_p]$ found in the corresponding equation of Ref. [16], which suggests that $[\omega_p]$ can have both the possible values, [2] and [11]. The reduced matrix elements $([n']\|z\|[n])$ are expressed as functions of n_1, n_2, and n_3 on p. 84 of Ref. [17]. The coefficients $c^{(p)}_{(\omega_o)}$ for $(p) = (s), (a)$ and $(\omega_o) = (11), (00)$, are given in Ref. [16]. The labels ρ and ρ' give the multiplicity in the coupling of the U(3) irreps $[\sigma]$ and $[n]$ to $[\omega]$, and $[\sigma']$ and $[n']$ to $[\omega']$.

The VCS techniques have successfully reduced the matrix elements in the complicated algebra of sp(6) to matrix elements in the simpler algebra of u(3). These matrix elements are expressed in terms of the $9(\lambda\mu)$ and Racah-U coefficients of U(3) which are easily obtained from existing codes [12], the i-space Racah coefficients of SU(2) and a few simple reduced matrix elements of the single-fermion creation and annihilation operators. The advantage of having an U(3) subgroup has thus been fully exploited. Moreover, the VCS method has provided us with expressions for the reduced matrix elements of operators with any I_p spin. We can therefore use the formulas in this section for the real quadrupole moment operator, which is not a generator of the sp(6)⊃u(3) algebra of the FDSM and includes operators with nonzero I_p spins.

III. POSSIBLE SU(3) IRREDUCIBLE REPRESENTATIONS

To perform detailed calculations for arbitrary proton and neutron numbers n in the actinide region, the possible SU(3) irreps in the sp(6) ⊃ u(3) group chain must be enumerated. Only the low generalized seniority states are of the greatest interest in the FDSM truncation scheme. Therefore, it is sufficient to list the possible SU(3) irreps as a function of n for Sp(6) irreps with $u \leq 2$. The quantum numbers that label the Sp(6) irreps are obtained from the highest weights which are the maximal eigenvalues of the Hermitian operators that form the Cartan subalgebra of Sp(6). These are expressed in terms of the intrinsic U(3) quantum numbers, $\sigma_1, \sigma_2, \sigma_3$ with $u = \sigma_1 + \sigma_2 + \sigma_3$, and the shell degeneracy quantum number Ω. In the $k - i$ basis of the FDSM,

$$\Omega = \sum_i \frac{1}{2}(2k+1)(2i+1) \tag{23}$$

and the Sp(6) irreps are labeled by $(\frac{\Omega}{3} - \sigma_3,\ \frac{\Omega}{3} - \sigma_2,\ \frac{\Omega}{3} - \sigma_1)$. The U(3) irreps $[\omega_1\omega_2\omega_3]$ for $n > u$ are then built starting with $n = u+2, u+4, \ldots$ through the U(3) coupling rules implied in Eq. (7). In this process forbidden states are recognized by constructing the $KK^\dagger$ matrices of Eq. (8) using the formulas in Ref. [16]. A zero denominator in the analytical expressions for one-dimensional $KK^\dagger$ matrices, or a zero eigenvalue for two- and three-dimensional $KK^\dagger$ matrices signals the occurrence of a forbidden state.

In this section, the allowed U(3) irreps $[\omega_1\omega_2\omega_3]$ for the $N = 6$ neutron shell are tabulated as functions of the neutron number n for Sp(6) irreps with $u = 0, 2$ in Tables I–III. The Elliott-SU(3) notation $(\lambda\mu)$ is used to label the states, where $\lambda = \omega_1 - \omega_2$, and $\mu = \omega_2 - \omega_3$. Tables I–III are labeled by the quantum numbers u, the single-particle normal parity states j for the $N = 6$ shell, the shell degeneracy Ω and the Sp(6) irrep. The SU(3) quantum numbers for the intrinsic state are also given when necessary, with $\lambda_\sigma = \sigma_1 - \sigma_2$ and $\mu_\sigma = \sigma_2 - \sigma_3$. Table I for the Sp(6) irrep $(\frac{\Omega}{3}, \frac{\Omega}{3}, \frac{\Omega}{3})$ with $u = 0$ gives the SU(3) irreps for all neutron numbers $0 \leq n \leq 42$. Tables II and III give the SU(3) irreps for the particle states up to the half-full shell with $n \leq 21$. The irreps for the hole states with $n > 21$ can be obtained from the particle states by particle-hole conjugation which replaces the quantum numbers $(\lambda\mu)$ by $(\mu\lambda)$. The superscripts in the tables give the number of occurrences of a particular $(\lambda\mu)$. The corresponding tables for the $N = 5$ proton shell are Tables 1, 3, and 4 of Ref. [14].

The most noteworthy features of these tables are the "Pauli holes" near the half-full shell where states with the largest values of the quantum numbers $(\lambda\mu)$ would have occurred without the Pauli exclusion principle and the fermion character of the pair constituents. It is this Pauli void which restricts the maximum $(\lambda\mu)$ value of (14 0) to occur at $n = 14$ for the $N = 6$ neutron shell and is responsible for the "fatal flaw" of Ginocchio. As mentioned in Sec. I, in order to obtain higher angular momentum states for highly deformed actinide nuclei, it may become necessary to mix shell model orbits from the $N = 7$ shell with those of the $N = 5$ shell and thus reach larger values of the SU(3) quantum numbers. The rather lengthy tables of possible SU(3) irreps for the mixed $N = 5, 7$ shell for the protons are given as Tables 5.9, 5.11, and

TABLE I. Possible $(\lambda\mu)$ for the $u = 0$ states of a $j = \frac{1}{2}\frac{3}{2}\frac{5}{2}\frac{7}{2}\frac{9}{2}\frac{11}{2}$ shell with $\Omega = 21$ and Sp(6) irrep $\equiv$ (777).

n	$(\lambda\mu)$												
42	(00)												
40	(02)												
38	(04)	(20)											
36	(06)	(22)	(00)										
34	(08)	(24)	(40)	(02)									
32	(0,10)	(26)	(42)	(04)	(20)								
30	(0,12)	(28)	(44)	(60)	(06)	(22)	(00)						
28	(0,14)	(2,10)	(46)	(62)	(08)	(24)	(02)	(40)					
26		(2,12)	(48)	(64)	(80)	(0,10)	(26)	(04)	(42)	(20)			
24			(4,10)	(66)	(82)	(0,12)	(28)	(06)	(44)	(22)	(00)	(60)	
22				(68)	(84)	(10,0)	(2,10)	(08)	(46)	(24)	(02)	(62)	(40)
20				(86)	(48)	(0,10)	(10,2)	(80)	(64)	(42)	(20)	(26)	(04)
18			(10,4)	(66)	(28)	(12,0)	(82)	(60)	(44)	(22)	(00)	(06)	
16		(12,2)	(84)	(46)	(08)	(10,0)	(62)	(40)	(24)	(02)			
14	(14,0)	(10,2)	(64)	(26)	(80)	(42)	(20)	(04)					
12	(12,0)	(82)	(44)	(06)	(60)	(22)	(00)						
10	(10,0)	(62)	(24)	(40)	(02)								
8	(80)	(42)	(04)	(20)									
6	(60)	(22)	(00)										
4	(40)	(02)											
2	(20)												
0	(00)												

5.12 in Ref. [15].

Only calculations for even particle numbers are considered in this work. The possible SU(3) irreps for $u = 1$ have been tabulated for the shells of interest as Table II in Ref. [14] and Tables 5.6 and 5.10 in Ref. [15]. This serves to illustrate that calculations for odd particle number can be performed in a similar manner and the FDSM assumptions for low-lying states of odd nuclei can also be studied.

IV. QUADRUPOLE MOMENT OPERATOR COEFFICIENTS

In order to do calculations in a truncated Sp(6) ⊃ U(3) basis, the operators to be used in the effective interaction Hamiltonian must be expanded in terms of irreducible tensor operators of the type introduced in Sec. II. As discussed in Sec. I, we will consider an effective interaction which includes a $Q\cdot Q$ term where Q is the real quadrupole moment operator. This operator, transformed to the $k-i$ basis of the FDSM, is a linear combination of the one-body operators similar to those of Eq. (18), and includes some whose values of I_p are not zero.

A. Coefficients of Q^2_μ in the $k-i$ basis

The standard form for the real dimensionless quadrupole moment operator is given by

$$Q^2_\mu = \frac{m\omega}{\hbar}\sum_{i=1}^{n} r_i^2\, Y^2_\mu(\theta_i,\phi_i). \tag{24}$$

TABLE II. Possible $(\lambda\mu)$ for the $u = 2$ states of a $j = \frac{1}{2}\frac{3}{2}\frac{5}{2}\frac{7}{2}\frac{9}{2}\frac{11}{2}$ shell with $(\lambda_\sigma\mu_\sigma) = (01)$,$\Omega = 21$ and Sp(6) irrep $\equiv$ (766).

n	$(\lambda\mu)$															
20								(94)	(11,0)	(67)	(75)	(56)	(83)	(91)	(72)	(29)
								(37)	(18)	(45)	(53)	(34)	(61)	(50)	(07)	(15)
								(23)	(31)	(12)	(01)					
18					(11,2)	(85)	(93)	(74)	(10,1)	(90)	(47)	(55)	(36)	(63)	(71)	(52)
					(09)	(17)	(25)	(33)	(14)	(41)	(30)	(03)	(11)			
16		(13,0)	(10,3)	(11,1)	(92)	(65)	(73)	(54)	(81)	(70)	(27)	(35)	(16)	(43)	(51)	(32)
		(05)	(13)	(21)	(10)											
14	(12,1)	(11,0)	(83)	(91)	(72)	(45)	(53)	(34)	(07)	(15)	(61)	(50)	(23)	(31)	(12)	(01)
12	(10,1)	(90)	(63)	(71)	(52)	(25)	(33)	(14)	(41)	(30)	(03)	(11)				
10	(81)	(70)	(43)	(51)	(32)	(05)	(13)	(21)	(10)							
8	(61)	(50)	(23)	(31)	(12)	(01)										
6	(41)	(30)	(03)	(11)												
4	(21)	(10)														
2	(01)															

TABLE III. Possible $(\lambda\mu)$ for the $u = 2$ states of a $j = \frac{1}{2}\frac{3}{2}\frac{5}{2}\frac{7}{2}\frac{9}{2}\frac{11}{2}$ shell with $(\lambda_\sigma\mu_\sigma) = (20)$,$\Omega = 21$ and Sp(6) irrep $\equiv (775)$.

n	$(\lambda\mu)$													
20									$(10,2)^2$	(86)	(94)	(91)	(37)	$(80)^2$	$(64)^3$
									$(26)^3$	(75)	(83)	(72)	(45)	$(48)^2$	(67)
									(56)	(53)	$(42)^3$	(61)	(34)	(31)	$(20)^2$
									(0,10)	(2,9)	(18)	(15)	$(04)^2$	(23)	(12)
18					(10,4)	(11,2)	(12,0)	(93)	$(82)^3$	(10,1)	$(66)^2$	(85)	(74)	(71)	(17)
					$(60)^2$	$(44)^3$	$(06)^2$	(55)	(63)	(52)	(25)	$(28)^2$	(47)	(36)	(33)
					$(22)^3$	(41)	(14)	(11)	(00)						
16			(12,2)	(10,3)	$(84)^2$	(11,1)	(92)	$(10,0)^2$	(73)	$(62)^3$	(81)	$(46)^2$	(65)	(54)	(51)
			$(40)^2$	$(24)^3$	(35)	(43)	(32)	(08)	(27)	(16)	(13)	$(02)^2$	(21)		
14		(12,1)	$(10,2)^2$	(83)	$(64)^2$	(91)	(72)	$(80)^2$	(53)	$(42)^3$	(61)	$(26)^2$	(45)	(34)	(31)
		$(20)^2$	$(04)^2$	(15)	(23)	(12)									
12	(12,0)	(10,1)	$(82)^2$	(63)	$(44)^2$	(71)	(52)	$(60)^2$	(33)	$(22)^3$	(41)	(06)	(25)	(14)	(11)
	(00)														
10	(10,0)	(81)	$(62)^2$	(43)	$(24)^2$	(51)	(32)	$(40)^2$	(13)	$(02)^2$	(21)				
8	(80)	(61)	$(42)^2$	(23)	(04)	(31)	(12)	$(20)^2$							
6	(60)	(41)	$(22)^2$	(11)	(00)										
4	(40)	(21)	(02)												
2	(20)														

This can be expressed in terms of nucleon creation and annihilation operators as

$$Q^2_\mu = \frac{m\omega}{\hbar}\sum_{n,l,j,m_j}\sum_{n',l',j',m_{j'}}\left\{\sqrt{\frac{5}{4\pi}}\left[\frac{1+(-1)^{l-l'}}{2}\right]\int_0^\infty dr r^2\, R^*_{Nl}(r)\, r^2\, R_{N'l'}(r)\right.$$
$$\left.\times\left\langle j\ \frac{1}{2}\ 2\ 0\ \middle|\ j'\ \frac{1}{2}\right\rangle\langle j'm_{j'}2\mu|jm_j\rangle a^\dagger_{n,l,\frac{1}{2},j,m_j}a_{n',l',\frac{1}{2},j',m_{j'}}\right\} \tag{25}$$

with even values for $l - l'$ within a major shell such as $N = 5$ or $N = 6$. The single-fermion creation and annihilation operators $a^\dagger_{jm_j}, a_{jm_j}$ of the shell model basis are written in terms of the pseudo-angular momenta k and i of the FDSM as Eqs. (1) and (2). Using standard angular momentum recoupling, the quadrupole moment operator is then written in the $k - i$ basis as

$$Q^2_\mu = \sum_{ii'K_pI_p} C_{ii'K_pI_p}[b^\dagger_{ki}\times\tilde{b}_{ki'}]_{[K_pI_p]2\mu}, \tag{26}$$

with $C_{ii'K_pI_p}$ given by

$$C_{ii'K_pI_p} = \frac{m\omega}{\hbar}\sqrt{\frac{1}{4\pi}}\left[\frac{1+(-1)^{l-l'}}{2}\right]\int_0^\infty dr r^2\, R^*_{Nl}(r)\, r^2\, R_{N'l'}(r)\times\left\langle j\ \frac{1}{2}\ 2\ 0\ \middle|\ j'\ \frac{1}{2}\right\rangle\sqrt{2j+1}\begin{bmatrix} k & i & j \\ k & i' & j' \\ K_p & I_p & 2\end{bmatrix}. \tag{27}$$

For $N' = N$ and $l' = l$, using $N = 2n + l$, the radial integral is

$$\int_0^\infty dr r^2\, R^*_{Nl}(r)\, r^2\, R_{Nl}(r) = N + \frac{3}{2}. \tag{28}$$

When the quantum numbers l' and l differ by 2, defining the larger (smaller) value as l_b (l_s), we get for $N' = N$,

$$\int_0^\infty dr r^2\, R^*_{Nl_b}(r)\, r^2\, R_{Nl_s}(r) = \mathcal{S}_{l_bl_s}\sqrt{(N+l_b+1)(N-l_s)}. \tag{29}$$

The phase factor $\mathcal{S}_{l_bl_s}$ with the value ±1, influences the magnitudes of the expansion coefficients of Q^2_μ in Eq. (26). The different combinations of $\mathcal{S}_{l'l}$ which result in different phase choices for the coefficients are given in Table IV. For the $N = 5$ shell, for example, with $l = 1, 3, 5$, there are four possible combinations of $\mathcal{S}_{l'l}$. This multiplicity arises because the relative signs of the radial wave functions R_{Nl} and $R_{Nl'}$ are quite arbitrary. For the $N = 5$ shell, we see from Table IV that the phase choice labeled phase 1 requires the value of both $\mathcal{S}_{31}$ and $\mathcal{S}_{53}$ to be positive. This corresponds to positive signs for R_{51}, R_{53}, and R_{55} as r goes to infinity and hence, alternating signs as r goes to zero. With the signs of

TABLE IV. The possible phase choices for the radial wave functions.

$N=5$	l	l'	$S_{l'l}$
Phase 1	1	3	+
	3	5	+
Phase 2	1	3	−
	3	5	−
Phase 3	1	3	+
	3	5	−
Phase 4	1	3	−
	3	5	+
$N=6$	l	l'	$S_{l'l}$
Phase 1	0	2	+
	2	4	+
	4	6	+
Phase 2	0	2	−
	2	4	−
	4	6	−
Phase 4	0	2	+
	2	4	+
	4	6	−
Phase 6	0	2	−
	2	4	+
	4	6	+

all three radial wave functions positive as r goes to zero, phase choice labeled Phase 2 is obtained. The other two possible phase choices are obtained from these two by changing the sign of R_{51} relative to the signs of R_{53} and R_{55}; thus phase 1 → phase 4 and phase 2 → phase 3. In the $k-i$ basis of the FDSM, the dependence on l and l' is implicit in the generation of the single-particle states. For the $N=5$ shell, in the k-active scheme with $k=1$, the single-particle states $j=\frac{1}{2}$ and $j=\frac{3}{2}$ are obtained with $i=\frac{1}{2}$. In the shell model basis these states have $l=1$. The single-particle states $j=\frac{5}{2}$, $\frac{7}{2}$, and $\frac{9}{2}$ are obtained in the $k-i$ basis with $i=\frac{7}{2}$, but in the shell model basis the states $j=\frac{5}{2}$ and $j=\frac{7}{2}$ have $l=3$ whereas the state $j=\frac{9}{2}$ has $l=5$. The relative signs of the states with different i are also arbitrary, therefore, the signs of the $i=\frac{1}{2}$ states can be reversed relative to those for $i=\frac{7}{2}$. This is equivalent to changing the sign of R_{51} relative to those of R_{53} and R_{55} which established the equivalence of phase 1 to phase 4, and phase 2 to phase 3.

For the $N=6$ shell, therefore, there are only four independent phase choices, instead of eight. These four are shown in Table IV. The remaining four labeled phase 3, 5, 7, and 8 can be obtained from these four by changing the phases for R_{64} and R_{66} relative to those for R_{62} and R_{60}. This is indeed equivalent to changing the sign of the $i=\frac{3}{2}$ states relative to those for the $i=\frac{9}{2}$ states in the $k-i$ basis.

The expansion coefficients of Q_μ^2 in the $k-i$ basis for the different values of i, i', K_p, I_p are tabulated without the factor $\sqrt{\frac{1}{4\pi}}$ in Tables V and VI for the $N=5$ and $N=6$ shells. Table V gives the coefficients for all four

TABLE V. The coefficients $C_{ii'K_pI_p}$ for the $N=5$ shell.

i	i'	K_p	I_p	Phase 1	Phase 2	Phase 3	Phase 4
$\frac{1}{2}$	$\frac{1}{2}$	2	0	−2.8406	−2.8406	−2.8406	−2.8406
$\frac{7}{2}$	$\frac{7}{2}$	0	2	−2.9442	−3.87411	−3.8741	−2.9442
$\frac{7}{2}$	$\frac{7}{2}$	1	1	−3.3162	−1.4566	−1.4566	−3.3162
$\frac{7}{2}$	$\frac{7}{2}$	1	3	−2.2004	−0.4162	−0.4162	−2.2004
$\frac{7}{2}$	$\frac{7}{2}$	2	0	1.8221	−1.1908	−1.1908	1.8221
$\frac{7}{2}$	$\frac{7}{2}$	2	2	1.8158	−3.1043	−3.1043	1.8158
$\frac{7}{2}$	$\frac{7}{2}$	2	4	−0.4343	−1.7190	−1.7190	−0.4343
$\frac{1}{2}$	$\frac{7}{2}$	1	3	2.2708	−2.2708	2.2708	−2.2708
$\frac{1}{2}$	$\frac{7}{2}$	2	3	1.6057	−1.6057	1.6057	−1.6057
$\frac{1}{2}$	$\frac{7}{2}$	2	4	1.6057	−1.6057	1.6057	−1.6057
$\frac{7}{2}$	$\frac{1}{2}$	1	3	−2.2708	2.2708	−2.2708	2.2708
$\frac{7}{2}$	$\frac{1}{2}$	2	3	1.6057	−1.6057	1.6057	−1.6057
$\frac{7}{2}$	$\frac{1}{2}$	2	4	−1.6057	1.6057	−1.6057	1.6057

phase choices. The equivalence of phase 1 and phase 4 as well as phase 2 and phase 3 can be seen explicitly. Table VI gives the coefficients only for the four independent phases of the $N=6$ shell. From these tables, it is clear that the overlap between a state vector in the shell model basis with specific values of l and l', and one in the $k-i$ basis with specific values of i and i' will be affected by the phase choice as determined by the signs of the radial wave functions R_{Nl} and $R_{Nl'}$. We have thus demonstrated the existence of more than one FDSM basis for a particular oscillator shell. This seems to have been overlooked by the founders of the FDSM, but has

TABLE VI. The coefficients $C_{ii'K_pI_p}$ for the $N=6$ shell.

i	i'	K_p	I_p	Phase 1	Phase 2	Phase 4	Phase 6
$\frac{3}{2}$	$\frac{3}{2}$	0	2	1.7241	−2.6423	1.7241	−2.6423
$\frac{3}{2}$	$\frac{3}{2}$	1	1	−5.0719	−0.7276	−5.0719	−0.7276
$\frac{3}{2}$	$\frac{3}{2}$	1	3	−0.3249	−2.3361	−0.3249	−2.3361
$\frac{3}{2}$	$\frac{3}{2}$	2	0	0.7933	−3.6821	0.7933	−3.6821
$\frac{3}{2}$	$\frac{3}{2}$	2	2	0.7386	−1.8578	0.7386	−1.8578
$\frac{9}{2}$	$\frac{9}{2}$	0	2	−4.5364	−0.5269	−0.5269	−4.5364
$\frac{9}{2}$	$\frac{9}{2}$	1	1	−3.4115	−1.5298	−1.5298	−3.4115
$\frac{9}{2}$	$\frac{9}{2}$	1	3	−2.4359	−0.6656	−0.6656	−2.4359
$\frac{9}{2}$	$\frac{9}{2}$	2	0	2.3638	−1.6334	−1.6334	2.3638
$\frac{9}{2}$	$\frac{9}{2}$	2	2	2.4329	−3.6215	−3.6215	2.4329
$\frac{9}{2}$	$\frac{9}{2}$	2	4	−0.2062	−1.8366	−1.8366	−0.2062
$\frac{3}{2}$	$\frac{9}{2}$	1	3	3.6758	−3.6758	3.6758	3.6758
$\frac{3}{2}$	$\frac{9}{2}$	2	3	1.3690	−1.3690	1.3690	1.3690
$\frac{3}{2}$	$\frac{9}{2}$	2	4	1.6190	−1.6190	1.6190	1.6190
$\frac{9}{2}$	$\frac{3}{2}$	1	3	−3.6758	3.6758	−3.6758	−3.6758
$\frac{9}{2}$	$\frac{3}{2}$	2	3	1.3690	−1.3690	1.3690	1.3690
$\frac{9}{2}$	$\frac{3}{2}$	2	4	−1.6190	1.6190	−1.6190	−1.6190

already been noted by Halse [8,9]. Neither the radial wave functions $R_{Nl}, R_{Nl'}$ nor the quantum numbers l, l' appear anywhere in the construction of the FDSM generators and the basis states.

It is also clear from these tables that the real Q^2_μ operator is very different from P^2_μ, the one-body operator with rank 2, used in the FDSM. The latter has nonzero coefficients only for entries with $i = i'$, $K_p = 2$, and $I_p = 0$, which would be proportional to $\sqrt{2i+1}$ as seen in Eq. (6). Tables V and VI show that these coefficients are by no means dominant in the real Q^2_μ operator.

B. The pseudo-SU(3) scheme

In the real SU(3) basis of Elliott, the $Q \cdot Q$ operator has a simple known eigenvalue. Nevertheless, a test of the calculations using $Q \cdot Q$ in the full untruncated shell model space for two particles, with FDSM basis states, cannot be performed since the FDSM basis is a truncated one. Only the normal-parity states with $j = \frac{1}{2}, \frac{3}{2}, \frac{5}{2}, \frac{7}{2}, \frac{9}{2}$ are included for the $N = 5$ shell with the $h_{\frac{11}{2}}$ orbit pushed down into the lower shell. Similarly, for the $N = 6$ shell, only the normal-parity states with $j = \frac{1}{2}, \frac{3}{2}, \frac{5}{2}, \frac{7}{2}, \frac{9}{2}, \frac{11}{2}$ are included in the FDSM with the $i_{\frac{13}{2}}$ orbit pushed down into the lower shell. However, the normal-parity states of the $N = 5$ and $N = 6$ shells are identical to those of the pseudo-oscillator shells with $\tilde{N} = 4$, $\tilde{l} = 0, 2, 4$; and $\tilde{N} = 5$, $\tilde{l} = 1, 3, 5$, respectively. The tildes are used to differentiate the pseudo-oscillator quantum numbers from the real oscillator quantum numbers. The pseudo-quadrupole moment operator $\tilde{Q}$ can also be expressed in the $k - i$ basis of the FDSM. Since the pseudo-SU(3) basis spans the same subspace of the shell model space as that of the FDSM, a diagonalization of $\tilde{Q} \cdot \tilde{Q}$ with known eigenvalues serves as a test in those cases when the full untruncated shell model space can be used in the FDSM.

C. Coefficients of $\tilde{Q}$ in the $k - i$ basis

For the $\tilde{N} = 4$ shell, the $b^\dagger$ operator is an $\tilde{l}$ space tensor belonging to the pseudo-SU(3) irrep (40) $\equiv$ [4]. Similarly, the $\tilde{b}$ is an $\tilde{l}$ space tensor belonging to the pseudo-SU(3) irrep (04) $\equiv$ [44]. For the $\tilde{N} = 5$ shell, these operators are $\tilde{l}$ space tensors belonging to the U(3) irreps [5] and [55], respectively. The pseudo-SU(3) quadrupole moment operator for a pseudo-oscillator shell, $\tilde{N}$, is obtained by coupling the $b^\dagger$ and $\tilde{b}$ operators and is given as

$$\tilde{Q}^2_\mu = c_{\tilde{l}_1\tilde{l}_2}[b^{\dagger[\tilde{N}]}_{\tilde{l}_1\,\frac{1}{2}} \times \tilde{b}^{[\tilde{N}\tilde{N}]}_{\tilde{l}_2\,\frac{1}{2}}]_{[\tilde{L}=2\tilde{S}=0]2\mu}, \tag{30}$$

where

$$c_{\tilde{l}_1\tilde{l}_2} = \langle (\tilde{N}0)\tilde{l}_1; (0\tilde{N})\tilde{l}_2 \| (11)2 \rangle. \tag{31}$$

This is transformed to the $k-i$ basis by angular momentum recoupling techniques to give

$$\tilde{Q}^2_\mu = \sum_{ii'K_pI_p} \tilde{c}_{ii'K_pI_p}[b^\dagger_{ki} \times \tilde{b}_{ki'}]_{[K_pI_p]2\mu} \tag{32}$$

with

$$\tilde{c}_{ii'K_pI_p} = \sum_{\tilde{l}_1\tilde{l}_2} \left\{ \langle (\tilde{N}0)\tilde{l}_1; (0\tilde{N})\tilde{l}_2 \| (11)2 \rangle \begin{bmatrix} \tilde{l}_1 & \tilde{l}_2 & 2 \\ \frac{1}{2} & \frac{1}{2} & 0 \\ j_1 & j_2 & 2 \end{bmatrix} \begin{bmatrix} k & i & j_1 \\ k & i' & j_2 \\ K_p & I_p & 2 \end{bmatrix} \right\}. \tag{33}$$

The only phase choice available in calculating the coefficients of $\tilde{Q}^2_\mu$ is implicitly made in the SU(3)-Wigner coefficient $\langle (\tilde{N}0)\tilde{l}_1; (0\tilde{N})\tilde{l}_2 \| (11)2 \rangle$ from the computer code of Draayer and Akiyama [12].

Since it has been shown that $\tilde{Q}^2_\mu$ and Q^2_μ have a large overlap [4] if properly normalized, the coefficients $\tilde{c}_{ii'K_pI_p}$ are not tabulated here. They can be found in Ref. [15], where it is also shown that the properly normalized coefficients $\tilde{C}_{ii'K_pI_p}$ defined by

$$\tilde{C}_{ii'K_pI_p} = \sqrt{\frac{5N(N+1)(N+2)(N+3)}{32\pi}}\,\tilde{c}_{ii'K_pI_p} \tag{34}$$

are such that $\tilde{C}_{ii'K_pI_p} \approx C_{ii'K_pI_p}$ for phase 1 in Tables V and VI. The coefficients of $\tilde{Q}^2_\mu$ and Q^2_μ for the $N = 5$ and $N = 6$ shells are not related exactly because of the differences in the FDSM and pseudo-SU(3) bases for these shells. However, a comparison of the two operators in this manner illustrates that they are effectively identical and serves as a check on the magnitude of the coefficients of Q^2_μ.

D. The $\tilde{Q} \cdot \tilde{Q}$ matrix

The $\tilde{Q} \cdot \tilde{Q}$ matrix has been calculated in the complete one- and two-particle basis of the FDSM. In order to verify that the states have been counted correctly, the states were also enumerated in the $\tilde{l} - \tilde{s}$ basis of the pseudo-SU(3) model. For the two-identical-particle case, the total spin is $\tilde{S} = 1$ or $\tilde{S} = 0$ corresponding to a spin symmetric or spin-antisymmetric wave function. The space wave functions are chosen to make the total wave function totally antisymmetric. The SU(3) irreps $(\lambda\mu)$ for the space wave functions are taken from the tables of Draayer and Leschber [18]. The values of $\tilde{L}$ are obtained for each $(\tilde{\lambda}\tilde{\mu})$ for the $\tilde{N} = 4$ and $\tilde{N} = 5$ shells using Elliott's rule [1]. The number of occurrences for each value of the total angular momentum $\tilde{J} \equiv J$ is obtained with $J = \tilde{L} \times \tilde{S}$. The diagonalization of the $\tilde{Q} \cdot \tilde{Q}$ matrix in the $k - i$ basis reproduces the correct number of occurrences for each value of J. The eigenvalues for each J, given by E_J, are explicitly expressed in terms of the eigenvalue of the Casimir operator of pseudo-SU(3), and the total

pseudo-orbital quantum number $\tilde{L}$. For

$$E_J = a\frac{2}{3}\left(\tilde{\lambda}^2+\tilde{\mu}^2+\tilde{\lambda}\tilde{\mu}+3(\tilde{\lambda}+\tilde{\mu})\right)-\frac{b}{2}\tilde{L}(\tilde{L}+1), \quad (35)$$

we get $a=b=\frac{1}{70}$ for the $\tilde{N}=4$ shell and $a=b=\frac{1}{140}$ for the $\tilde{N}=5$ shell. The eigenvalues of the $\tilde{Q}\cdot\tilde{Q}$ matrix for two particles are reproduced correctly. It is interesting to note that the quantum numbers $\tilde{\lambda},\tilde{\mu}$ for the two-particle spaces in the $\tilde{N}=4$ and $\tilde{N}=5$ shells are much larger than the λ,μ values of the FDSM-SU(3) symmetry. For the $N=5$ shell, Tables III and IV of Ref. [14] show that λ and μ are ≤ 2 when $n=2$. The same is true for the $N=6$ shell as seen in Tables II and III of this work. We also verified that the eigenvalues of the $\tilde{Q}\cdot\tilde{Q}$ matrix for a single particle describe a rotational energy spectrum for both shells.

The self-consistency checks described above have verified the values of the expansion coefficients of $\tilde{Q}^2_\mu$, the number of occurrences for a particular J, and the eigenvalues of the $\tilde{Q}\cdot\tilde{Q}$ matrix for a one- and two-particle calculation. The tests validate all the analytical expressions of Sec. II which were used in the calculation as well as the computer codes that evaluate the numerical results. The success of the tests lends credibility to the results of the two-particle calculations with the real $Q\cdot Q$ matrix, which is presented in the following section.

V. GENERALIZED SENIORITY MIXING IN THE TWO-PARTICLE STATES

In this section we describe a complete two-particle calculation using a modified FDSM Hamiltonian as a first step in studying the FDSM assumptions. Our calculation is performed for (i) two valence protons and (ii) two valence neutrons which, for actinide nuclei are assigned to the $N=5$ and $N=6$ shells, respectively, in the k-active scheme of the FDSM.

We begin by compiling the dictionary of allowed SU(3) irreps for two-particle states in the $k-i$ basis expanded in terms of the generalized seniority states with $u=0$ and $u=2$.

A. Dictionary of two-particle states

The single particle $j=\frac{1}{2},\frac{3}{2},\frac{5}{2},\frac{7}{2},\frac{9}{2}$ states of the $N=5$ shell are obtained in the k-active scheme of the FDSM with $k=1$ and $i=\frac{1}{2},\frac{7}{2}$. The two-particle states for $u=0$ and $u=2$ are labeled as $|[[n]\times[\sigma]][\omega];\ K;(i_1i_2)I;JM\rangle$. The $u=0$ state with $[\sigma]=[0],[n]=[\omega]=[2];K=0$ or 2 is the coherent superposition of states with $i_1=i_2$ and $I=0$ whose coefficients are proportional to $\sqrt{i_1+\frac{1}{2}}$. The $u=2$ state with $[\sigma]=[\omega]=[2],[n]=[0]$ and $K=0$ or 2, includes states with $(i_1i_2)I$ combinations of $(\frac{1}{2}\frac{1}{2})I=0$, $(\frac{7}{2}\frac{7}{2})I=0,\ 2,\ 4,\ 6$, and $(\frac{1}{2}\frac{7}{2})I=3,\ 4$ while the $u=2$ state with $[\sigma]=[\omega]=[11],[n]=[0]$ and $K=1$, includes states with $(i_1i_2)I$ combinations of $(\frac{1}{2}\frac{1}{2})I=1$, $(\frac{7}{2}\frac{7}{2})I=1,\ 3,\ 5,\ 7$, and $(\frac{1}{2}\frac{7}{2})I=3,\ 4$. Note that the two-particle state with $u=2$ and $I=0$ involves a linear combination

$$|u=2\rangle = -\sqrt{\frac{4}{5}}\left|\frac{1}{2}\frac{1}{2}\right\rangle+\sqrt{\frac{1}{5}}\left|\frac{7}{2}\frac{7}{2}\right\rangle. \quad (36)$$

This state, given with only the i_1i_2 values, is orthogonal to the $u=0$ state with the same $[\omega]$, K, I quantum numbers.

For the $N=6$ shell with $j=\frac{1}{2},\frac{3}{2},\frac{5}{2},\frac{7}{2},\frac{9}{2},\frac{11}{2}$, the i values are $i=\frac{3}{2},\frac{9}{2}$ in the k-active scheme of the FDSM with $k=1$. The $u=0$ state is identical to that for the $N=5$ shell. The $u=2$ states now have $[\sigma]=[\omega]=[2],[n]=[0]$ and $K=0$ or 2, with $(i_1i_2)I$ combinations of $(\frac{3}{2}\frac{3}{2})I=0,\ 2$, $(\frac{9}{2}\frac{9}{2})I=0,\ 2,\ 4,\ 6,\ 8$, and $(\frac{3}{2}\frac{9}{2})I=3,\ 4,\ 5,\ 6$, or $[\sigma]=[\omega]=[11],[n]=[0]$ and $K=1$, with $(i_1i_2)I=(\frac{3}{2}\frac{3}{2})1,\ 3$, $(\frac{9}{2}\frac{9}{2})3,\ 5,\ 7,\ 9$, and $(\frac{3}{2}\frac{9}{2})3,\ 4,\ 5,\ 6$. Again, the two-particle state with $u=2$ and $I=0$ involves a linear combination

$$|u=2>= -\sqrt{\frac{5}{7}}\left|\frac{3}{2}\frac{3}{2}\right\rangle+\sqrt{\frac{2}{7}}\left|\frac{9}{2}\frac{9}{2}\right\rangle. \quad (37)$$

which is orthogonal to the $u=0$ state.

B. The Hamiltonian

The Hamiltonian used for the two-particle calculation is

$$\frac{H}{V_0} = -[(1-g)Q\cdot Q+g(S^\dagger S+\mathbf{D}^\dagger\mathbf{D})]. \quad (38)$$

1. *Construction of the $Q\cdot Q$ matrix*

With $Q\cdot Q=\sum_\mu Q^2_\mu Q^2_{-\mu}(-1)^\mu$, and α designating the (i_1i_2) structure of the states, the $Q\cdot Q$ matrix can be put in the form

$$\begin{aligned}\langle[[n']\times[\sigma']][\omega'];\alpha'[K'\times I']J'M'|Q\cdot Q|[[n]\times[\sigma]][\omega];\alpha[K\times I]JM\rangle \\ = \sum_{[\bar{n}][\bar{s}][\bar{\omega}]}\sum_{\bar{\alpha}\bar{K}\bar{I}\bar{J}}\{\langle[[n']\times[\sigma']][\omega'];\alpha'[K'\times I']J'\|Q^2\|[[\bar{n}]\times[\bar{s}]][\bar{\omega}];\bar{\alpha}[\bar{K}\times\bar{I}]\bar{J}\rangle \\ \times\langle[[n]\times[\sigma]][\omega];\alpha[K\times I]J\|Q^2\|[[\bar{n}]\times[\bar{s}]][\bar{\omega}];\bar{\alpha}[\bar{K}\times\bar{I}]\bar{J}\rangle\}, \quad (39)\end{aligned}$$

where the Wigner-Eckart theorem has been used after the introduction of a sum over the complete set of intermediate

states. Angular momentum recoupling is also used to uncouple the quantum numbers K, I, J in the initial and intermediate states, and in the operator. The double-barred angular momentum-reduced matrix elements of Eq. (39) are further reduced to triple-barred matrix elements of the type defined in Sec. II. Finally, after identifying the U(3) character of Q^2 specifically, we write these double-barred matrix elements as follows

$$\langle[[n]\times[\sigma]][\omega];\alpha[K\times I]J\|Q^{2[\omega_o]}_{[K_p\times I_p]J_p}\|[[\bar{n}]\times[\bar{s}]][\bar{\omega}];\bar{\alpha}[\bar{K}\times\bar{I}]\bar{J}\rangle$$

$$=\langle[[n]\times[\sigma]][\omega];\alpha I\|Q^2_{I_p}\|[[\bar{n}]\times[\bar{s}]][\bar{\omega}];\bar{\alpha}\bar{I}\rangle\langle[\bar{\omega}]\bar{K};[\omega_o]K_p||[\omega]K\rangle\langle[1]1;[11]1||[\omega_o]K_p\rangle\begin{bmatrix}\bar{K}&\bar{I}&\bar{J}\\K_p&I_p&2\\K&I&J\end{bmatrix}. \quad (40)$$

The triple-barred matrix element of Q in Eq. (40) is calculated using the expressions for the triple-barred matrix elements in the VCS method given for example, by Eq. (21). The SU(3) $\supset$ SO(3) Wigner coefficients in Eq. (40) include the coefficient $\langle[1]1;[11]1||[\omega_o]K_p\rangle$ which is needed to convert the one-body operator Q of Eq. (26) from a spherical tensor in k space to a U(3) irreducible tensor.

The analytical expressions given above and the corresponding computer codes have been tested by diagonalizing the $P^2\cdot P^2$ matrix with the generators P^2 defined in Eq. (6). The numerical values obtained using these complicated formulas for the reduced matrix elements are identical to the eigenvalues given by Eq. (35) with a and b equal to 1, and $\tilde{L}$ replaced by K.

2. Construction of the $S^\dagger S$ and $D^\dagger\cdot D$ matrices

The $S^\dagger, S$ and $D^\dagger, D$ operators are special cases of the pair-creation operator $A^\dagger$ and the pair-annihilation operator A given by Eqs. (15) and (16). The initial and final states for the matrix elements of these generators are the same, i.e., the U(3) irreps $[n]=[n']$, $[\sigma]=[\sigma']$, and $[\omega]=[\omega']$. The expression for the reduced matrix element of $A^\dagger$ is given by Eq. (30) of Ref. [14]. Including the normalization factor of $\sqrt{\frac{3}{4}}$ to be consistent with the FDSM definitions and using the procedure discussed above for the matrix elements of $Q\cdot Q$, we get the matrix elements of the two-body operator $A^\dagger\cdot A$ as follows:

$$\langle[[n]\times[\sigma]][\omega];\alpha[K\times I]JM|A^\dagger\cdot A|[[n]\times[\sigma]][\omega];\alpha[K\times I]JM\rangle$$

$$=\sum_{[\bar{n}][\bar{\omega}]\bar{K}\bar{J}}\left\{\frac{3}{4}(\Lambda_{[n][\omega]}-\Lambda_{[\bar{n}][\bar{\omega}]})\langle[n]\|z\|[\bar{n}]\rangle^2\langle[1]1;[1]1\|[2]K_p\rangle^2\right.$$

$$\left.\times\langle[\bar{\omega}]\bar{K};[2]K_p\|[\omega]K\rangle^2U^2([\bar{\sigma}][\bar{n}][\omega][2];[\bar{\omega}][n])\begin{bmatrix}\bar{K}&I&\bar{J}\\K_p&0&K_p\\K&I&J\end{bmatrix}^2\right\}. \quad (41)$$

For the calculation of the $S^\dagger S$ matrix, the value of K_p is 0 and for the $\mathbf{D}^\dagger\cdot\mathbf{D}$ matrix it is 2. The value of $(\Lambda_{[n][\omega]}-\Lambda_{[\bar{n}][\bar{\omega}]})$ is given by Eq. (20) of Ref. [14]. Since the $S^\dagger, S$ and $D^\dagger, D$ operators are generators, the combination $S^\dagger S+\mathbf{D}^\dagger\cdot\mathbf{D}$ can be expressed in terms of the Casimir operator of Sp(6), the Casimir operator of SU(3), the number operator, and the shell degeneracy quantum number Ω given by Eq. (23). The numerical results of the computer codes and the complicated formulas of Eq. (41) needed to calculate the pure $S^\dagger S$, or $\mathbf{D}^\dagger\cdot\mathbf{D}$ term are therefore verified against the values obtained from this simpler form for the matrix elements of $S^\dagger S+\mathbf{D}^\dagger\cdot\mathbf{D}$.

C. Results of seniority mixing for two particles

In the FDSM, the favored $S^\dagger$, S and $\mathbf{D}^\dagger$, $\mathbf{D}$ pairs appear on an equal footing. FDSM Hamiltonians usually include the scalar product of these generators of the sp(6) algebra as well as a $P\cdot P$ term, where the P-type operators are the generators of the u(3) subalgebra. In the Hamiltonian given in Eq. (38), the P operator of Eq. (6) is replaced by the real quadrupole moment operator Q^2_μ defined in Eqs. (26) and (27). This operator connects the generalized seniority states $u=0$ and $u=2$, since it includes some P-type operators whose values of I_p are not zero. Therefore, an assessment of the seniority mixing between states with $u=0$ and states with $u=2$ can be made by diagonalizing the Hamiltonian of Eq. (38). We have quantified our assessment by computing the percentage of the $u=0$ components for the lowest $J=0$ and the lowest $J=2$ two-particle eigenstates The results are given as a function of the strength of the quadrupole moment operator contribution, $1-g$. With the coupling strength g ranging from 0.0 to 1.0, we can analyze the seniority mixing for the two extreme cases; with $g=0.0$, only the $Q\cdot Q$ term in the Hamiltonian gives a contribution whereas with $g=1.0$ only the pairing terms do. A

TABLE VII. Percentage of $u = 0$ for the lowest $J = 0, 2$ eigenstates in the $N = 5$ shell.

$1-g$	$J=0$	$J=2$ Phase 1	$J=2$ Phase 2
0.0	100	100	100
0.2	96.5	97.5	95.1
0.4	86.8	26.7	59.1
0.6	75.8	4.9	24.7
0.8	66.6	2.8	14.6
1.0	59.9	2.1	10.9

specific value of the potential V_0 is not chosen here. It is introduced in Eq. (38) in order to make the Hamiltonian dimensionless.

The dependence of seniority mixing on the relative phases of the radial wave functions with different l quantum numbers is also shown. For one particle, the eigenvalues and eigenvectors obtained after diagonalizing the $Q\cdot Q$ matrix are the same irrespective of the phase choice. For two particles, the eigenvalues are independent of the choice of phase for all J, but the coefficients of the $k-i$ basis vectors in the eigenstates are independent of the phase choice only for $J = 0$. The total spin for the two particles, each with spin $s = \frac{1}{2}$, is $S = 0$ or $S = 1$. In order to get a total J value of $J = 0$, we have two choices. Either the total orbital angular momentum, L and S both have a value of 0 or both have a value of 1. The value of $L = 0$ can be obtained only if l and l' are equal. However, a multiplicity in the choice of phase is available only if l and l' differ by 2, in which case they also cannot give a resultant value of $L = 1$. Therefore, the results for the $J = 0$ eigenstate are independent of the relative phases of the radial wave functions. The second column of Tables VII and VIII contain the results for the $J = 0$ eigenstate for the $N = 5$ and $N = 6$ shell, respectively. The third (fourth) column of Table VII contains the percentage of the $u = 0$ components in the lowest $J = 2$ eigenstate for the $N = 5$ shell when the coefficients of Q^2_μ labeled phase 1 (phase 2) in Table V are used in the calculation. The percentage of the $u = 0$ components in the lowest $J = 2$ eigenstate for the four independent phase choices for the $N = 6$ shell are tabulated in the last four columns of Table VIII.

The effective interaction of Eq. (38) is a reasonable one for testing the validity of the FDSM assumptions since it simulates the more traditional $J = 0$ pairing plus quadrupole-quadrupole interaction of Kumar and Baranger [19], and also incorporates the favored-pair operators of the FDSM. A two-particle state with $u = 0$ and $J = 2$ can be created only by a $D^\dagger$ pair operator. The matrix elements of the $\mathbf{D}^\dagger\cdot\mathbf{D}$ operator are the diagonal matrix elements of the Hamiltonian of Eq. (38) with both the initial and final states having values of $u = 0$ and $J = 2$. The off-diagonal matrix elements between the $u = 0, J = 2$ and $u = 2, J = 2$ states come from the $Q\cdot Q$ term in Eq. (38). On the other hand, the $S^\dagger$ operator can only make a two-particle state with $u = 0$ and $J = 0$. If a Hamiltonian with only the $S^\dagger S$ and $Q\cdot Q$ terms is diagonalized for a two-particle system, the eigenvalues and eigenvectors with $J = 0$ are identical to those for the full Hamiltonian of Eq. (38). This is because the $\mathbf{D}^\dagger\cdot\mathbf{D}$ term makes no contribution to the $J = 0$ matrix. The seniority mixing for such a Hamiltonian for the lowest $J = 0$ eigenstate is still given by the $J = 0$ column of Tables VII and VIII. For any $J \neq 0$ matrix, on the other hand, the $S^\dagger S$ term makes no contribution in the two-particle calculation, and a Hamiltonian with a pairing term of pure $S^\dagger S$ type contributes only through the $Q\cdot Q$ term. The percentages for the $u = 0$ states in the lowest $J = 2$ eigenstates are thus given by the entries for $g = 0.0$ in the $J = 2$ columns of Tables VII and VIII. We see that the $u = 0$ components in the lowest $J = 2$ eigenstates are less than 10.9% for all possible phases for this Kumar and Baranger type of effective interaction. The high $u = 0$ percentages for the $J = 0$ eigenstates serve only to confirm that the favored S pair of the FDSM is very close to the S pair in the shell model $j-j$ basis. It is the "realistic" nature of the favored D pair with $J = 2$ that is appraised in this section.

Now consider the results for $1-g = 0.4$ in the $N = 5$ shell for a moderate FDSM pairing interaction combined with a $Q\cdot Q$ interaction. The choice of basis labeled phase 2 gives 59.1% $u = 0$ components in the lowest $J = 2$ eigenstates. The other choice gives an even poorer result of 26.7%. The case for the $N = 6$ shell is also not very strong since, among the four possible choices for a basis, the highest percentage is only 50%. For both protons and neutrons of actinide nuclei, as the value of $1-g$ increases (indicating stronger quadrupole strengths and therefore stronger seniority mixing), we see that the percentage of the $u = 0$ components decreases.

The two-particle calculation presented in this section has shown that the $u \neq 0$ components are significantly large when an FDSM pairing plus real quadrupole-quadrupole interaction is diagonalized in the *complete* two-particle basis expanded in terms of generalized seniority states. The evidence for strong generalized seniority mixing which is seen here indicates that the low-lying states of even nuclei are *not* predominantly states with $u = 0$ made entirely from the favored S, D pairs of the FDSM. If they were, then the overlap between the lowest $J = 2$ eigenstates in the FDSM truncated basis which is a subspace of the shell model basis, and the complete shell model basis ($u = 0$ and $u = 2$) for two particles would be close to unity.

TABLE VIII. Percentage of $u = 0$ for the lowest $J = 0, 2$ eigenstates in the $N = 6$ shell.

$1-g$	$J=0$	$J=2$ Phase 1	$J=2$ Phase 2	$J=2$ Phase 4	$J=2$ Phase 6
0.0	100	100	100	100	100
0.2	96.4	95.7	95.1	98.4	95.4
0.4	85.6	26.3	50	15	40
0.6	72.5	6.8	20.4	1.5	10.7
0.8	61.8	4.1	12.1	0.8	6.2
1.0	54.1	3.2	10	0.6	4.6

VI. THE NATURE OF THE FDSM-SU(3) SYMMETRY

An ideal truncation scheme would have been based on S and D fermion pairs which create two-particle states very similar to the lowest $J = 0$ and $J = 2$ eigenstates in a two-particle system. However, it has been argued [10] that a good test of the validity of a truncation scheme cannot be made in a two-identical-particle system since it is thought to be noncollective in nature. As a next test of the FDSM, we therefore turn to (i) a system of ten protons in the $N = 5$ shell and (ii) a system of fourteen neutrons in the $N = 6$ shell. Both are identical-particle systems for actinide nuclei and contain the largest possible values of the FDSM-SU(3) quantum numbers, i.e., (10 0) for the protons and (14 0) for the neutrons. Their potential for greater collectivity is thus established. If the FDSM basis with its SU(3) symmetry is a good one for collective states, we would expect an effective interaction with a large $Q \cdot Q$ component to drive these most collective SU(3) irreps to be the dominant components in the lowest eigenstates of the ten-proton and fourteen-neutron systems. Since even the $u = 0$ Sp(6) irreps contain a fairly rich combination of both large and small SU(3) quantum numbers, a calculation in the truncated FDSM basis consisting of the pure $u = 0$ states should be sufficient for this purpose. The conclusions based on such a calculation for ten protons and fourteen neutrons could only be reinforced by the inclusion of the $u = 2$ states, since these states contain many SU(3) irreps with smaller values of the SU(3) quantum numbers than the $u = 0$ states.

A. Dictionary of basis states

The SU(3) irreps for the states with $u = 0$ for ten protons are chosen from Table 1 of Ref. [14]. They are (10 0), (62), (24), (40), and (02). For $u = 2$, with $(\lambda_\sigma \mu_\sigma) = (01)$, the states chosen from Table 3 of Ref. [14] are (81), (70), (43), (51), (32), (05), (13), (21), (10), and with $(\lambda_\sigma \mu_\sigma) = (20)$, the states chosen from Table 4 of Ref. [14] are (81), $(62)^2$, (43), (51), $(24)^2$, $(40)^2$, (32), (13), $(02)^2$, (21). The SU(3) irreps for the states with $u = 0$ for fourteen neutrons ($n = 14$) are chosen from Table I. For $u = 2$, with $(\lambda_\sigma \mu_\sigma) = (01)$ and (20), the states are chosen from Tables II and III, respectively.

B. The Hamiltonian

The Hamiltonian used for both the proton and the neutron calculation is

$$\frac{H}{V_0} = -[(1-g)Q \cdot Q + g(S^\dagger S)]. \tag{42}$$

The calculation of the matrix elements for the operators in the Hamiltonian proceeds in the same manner as for two particles. The main difference is that the K and K^{-1} matrices of Eq. (19) are no longer one dimensional. The quantum number ν has two values when two different irreps $[n]$ couple to $[\sigma] = [2]$ to give the same $[\omega]$. The matrices are then explicitly constructed using Eqs. (12) and (13). We have verified the computer codes and the expressions for the matrix elements of $P^2 \cdot P^2$ and of $S^\dagger S + \mathbf{D}^\dagger \cdot \mathbf{D}$ which they evaluate, in an analogous manner to the two-particle case. However, the test of the matrix elements of $Q \cdot Q$ using the pseudo-SU(3) model cannot be performed since the pseudo-SU(3) basis no longer spans the same subspace of the shell model space as the truncated $k - i$ basis for the ten-proton or fourteen-neutron calculation.

C. Results

The values of $1 - g$ for which the calculations were performed range from 0.0 to 1.0 in increments of 0.2. Our motivation to use the interaction of Eq. (42) comes from the work of Kumar and Baranger [19], who used the $J = 0$ pairing plus $Q \cdot Q$ interaction to study the competition between the shell model and the collective rotational model for nuclei with increasing numbers of valence protons and neutrons. A comparison of the coupling strengths of the operators in the interaction of Eq. (42) with those used by Kumar and Baranger for actinide nuclei, gives a value of $1 - g$ equal to 0.11 for the protons and 0.13 for the neutrons. These two additional points have also been calculated explicitly.

Although we have chosen a truncated basis consisting only of states with $u = 0$, the states with $u = 2$ enter into the picture as intermediate states in the calculation of the off-diagonal matrix elements of Q^2_μ, which in turn contribute to the matrix elements of $Q \cdot Q$. The large values for such off-diagonal matrix elements in our calculations are an indirect signal that if the states with $u = 2$ were permitted, their contributions to the eigenstates would be large. Note also that the effect of the phase choice for the radial wave functions is seen not only in the eigenvectors but also in the eigenvalues for all J. This is because we are no longer dealing with a complete basis as we did for the two-particle calculation.

The most important result which we present here addresses the assumption made in the FDSM that the lowest eigenstates of even nuclei have the largest SU(3) quantum numbers $(\lambda\mu)$. This cannot be done with the two-particle calculation, since only one SU(3) irrep is available for the state with $u = 0$. On the other hand, five different SU(3) irreps are available in the truncated basis for ten protons in the $N = 5$ shell and eight for fourteen neutrons in the $N = 6$ shell. The Hamiltonian in Eq. (42) is diagonalized in this richer basis and the percentage of different basis states in the resulting eigenstates is computed. For the ten-proton system, the eigenvalues of the Casimir operator of SU(3) are $\frac{2}{3}(130)$, $\frac{2}{3}(76)$, $\frac{2}{3}(46)$, $\frac{2}{3}(28)$, and $\frac{2}{3}(10)$ for $(\lambda\mu)$=(10 0), (62), (24), (40), and (02), respectively. If the FDSM-SU(3) symmetry leads to collectivity and rotational spectra in the same way as Elliott's SU(3) symmetry, we would expect the lowest eigenstates to be dominated by the basis state with the SU(3) irrep (10 0) and a $J = 0$, 2, 4, 6, 8, 10 rotational band structure. This would be followed at higher

energies by bands with dominant $(\lambda\mu) = (62)$, (24), (40), and (02) characteristics. Similar conclusions would hold for the fourteen-neutron system.

In Fig. 1 we present the percentage of basis states in the three lowest eigenstates of $J = 0$ as a function of $1-g$ for ten protons in the $N = 5$ shell. The coefficients of Q^2_μ labeled phase 1 in Table V are used in calculating the $Q \cdot Q$ matrix. The basis states are labeled by the SU(3) irreps. For the lowest eigenstate, the contribution of the state with (10 0) is close to 0% for all values of $1 - g$. For the second lowest eigenstate, the contribution of the state with (62) is not the dominant one for any value of $1 - g$. For the third lowest eigenstate, the state with (24) becomes the dominant component only for values of $1 - g$ greater than 0.5. The scenario is very similar in Fig. 2 where the coefficients of Q^2_μ labeled phase 2 in Table V are used to calculate the $Q \cdot Q$ matrix. For the lowest eigenstate, the results are almost identical to that of Fig. 1. The percentages of the state with (62) in the second lowest eigenstate and the state with (24) in the third lowest eigenstate are smaller than for phase 1, increasing only when $1 - g$ is greater than 0.7. In Figs. 3 and 4 the results for fourteen neutrons in the $N = 6$ shell are presented for two of the four possible phases for the coefficients in Table VI. We plot the percentage of the basis states labeled with six of the eight possible SU(3) irreps. For the lowest eigenstate in both phases, the contribution of the state with (14 0) is close to 0%. For the second lowest eigenstate the contribution for the

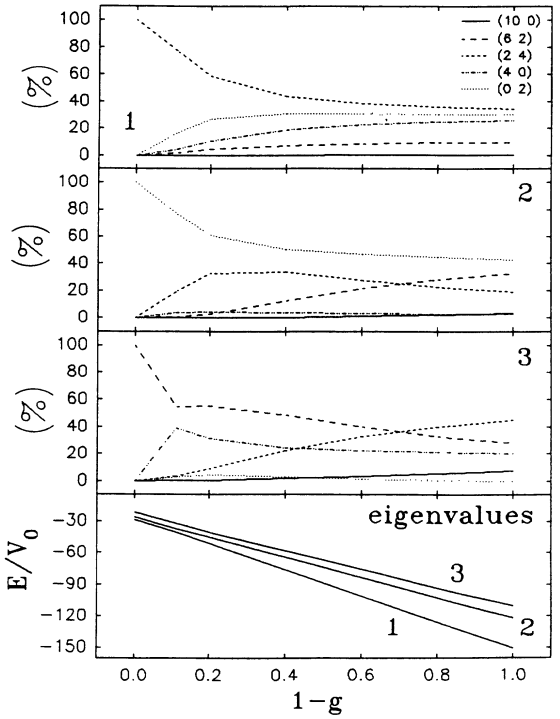

FIG. 2. Using phase 2 for the $N = 5$ shell, the percentage of basis states in the lowest $J = 0$ eigenstate (plot labeled 1), the second-lowest eigenstate (plot labeled 2) and the third-lowest eigenstate (plot labeled 3). The corresponding three lowest $J = 0$ eigenvalues are shown in the plot labelled eigenvalues.

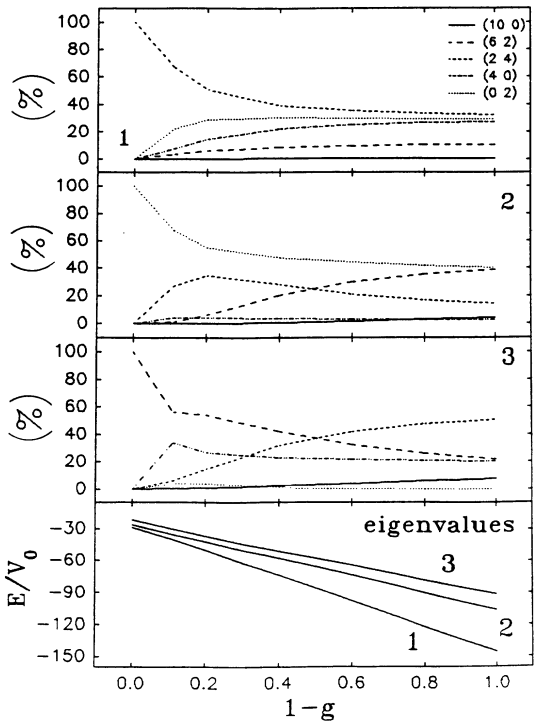

FIG. 1. Using phase 1 for the $N = 5$ shell, the percentage of basis states in the lowest $J = 0$ eigenstate (plot labeled 1), the second-lowest eigenstate (plot labeled 2) and the third-lowest eigenstate (plot labeled 3). The corresponding three lowest $J = 0$ eigenvalues are shown in the plot labeled eigenvalues.

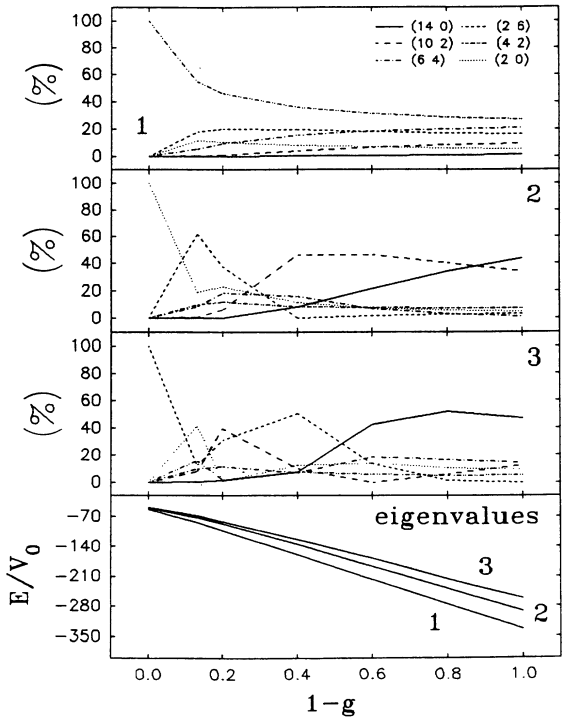

FIG. 3. Using phase 1 for the $N = 6$ shell, the percentage of basis states in the lowest $J = 0$ eigenstate (plot labeled 1), the second-lowest eigenstate (plot labeled 2) and the third-lowest eigenstate (plot labeled 3). The corresponding three lowest $J = 0$ eigenvalues are shown in the plot labeled eigenvalues.

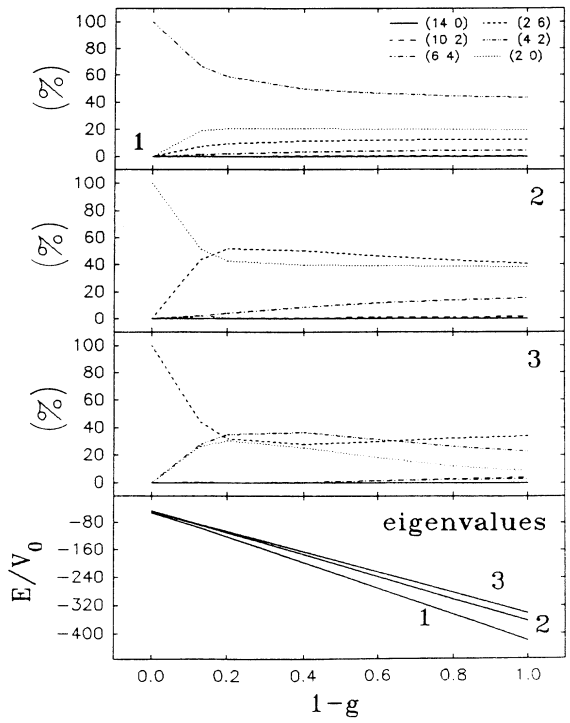

FIG. 4. Using phase 2 for the $N = 6$ shell, the percentage of basis states in the lowest $J = 0$ eigenstate (plot labeled 1), the second-lowest eigenstate (plot labeled 2), and the third-lowest eigenstate (plot labeled 3). The corresponding three lowest $J = 0$ eigenvalues are shown in the plot labeled eigenvalues.

state with (10 2) is dominant for values of $1 - g$ between 0.3 and 1.0 for phase 1, but very close to 0% for all values of $1 - g$ for phase 2. For the third lowest eigenstate the state with (64) is not the dominant component for either choice of phase. For both protons and neutrons the results for phase 2 are slightly worse than that for phase 1. The other phase choices for the neutrons also give similar results. For both protons and neutrons, the results for the $J \neq 0$ eigenstates are equally unfavorable.

From the results presented in this section we conclude that the SU(3) symmetry in the eigenstates of our interaction in the FDSM basis is completely different from that of Elliott's SU(3) symmetry. The lowest states of even nuclei do not have the largest SU(3) quantum numbers as assumed in the FDSM. The phenomenological validity of Elliott's SU(3) symmetry lies in a large correspondence between wave functions in Elliott's scheme and those in the shell model associated with observed rotational bands. The SU(3) content of our eigenstates have no correspondence with those obtained in Elliott's scheme. Therefore, the rotational feature of the FDSM-SU(3) symmetry for both the protons and the neutrons of actinide nuclei is subject to question.

The SU(3) symmetry arises in the FDSM through the $P^2 \cdot P^2$ term, where P^2 is one of the generators of the u(3) algebra in the k-active scheme. The eigenvalue of this operator is

$$E(P^2 \cdot P^2) = E(C^{\mathrm{SU}(3)}) - \frac{1}{2}K(K+1). \tag{43}$$

This operator plays the role of the quadrupole-quadrupole interaction in the FDSM Hamiltonians. Appropriate attractive values of the coupling strength for this operator will guarantee that FDSM Hamiltonians in the truncated basis of states with $u = 0$ give eigenstates which exhibit an Elliott-type SU(3) symmetry. Since the FDSM space is a subspace of the full shell model space, one could expect these to be the eigenstates of a shell model interaction. The interaction we have used is a first approximation towards a reasonable effective interaction for the shell model. However, the SU(3) irreps of the eigenstates which result from diagonalizing this interaction do not have the order dictated by a collective-SU(3) scheme. Clearly, the two sets of eigenstates are very different. This implies that a drastic renormalization of shell model effective interactions is necessary before they can be used in the truncated space.

VII. THE COUPLED PROTON-NEUTRON SYSTEM

In the n-identical-particle calculations discussed earlier, we tested the FDSM assumptions in the proton and neutron bases separately. Since quadrupole collectivity in nuclei depends on cooperative effects involving both protons and neutrons, the next logical step is to diagonalize an effective interaction which includes a coupled proton-neutron quadrupole interaction in a strongly-coupled proton-neutron basis.

In view of the results of Sec. VI, we would not expect the low-lying states of the coupled proton-neutron system to be dominated by high SU(3) quantum numbers without a drastic renormalization in the separate proton and neutron bases. For this reason we have chosen to force the proton and neutron SU(3) representations to be pure (10 0) and (14 0) representations and neglect all other components completely. This will still permit us to answer the question: Does an effective interaction with a strong attractive proton-neutron $Q \cdot Q$ component drive the coupled proton-neutron system into the most collective SU(3) representations with well established rotational band structure? The basis states for the coupled twenty-four-particle system are thus obtained by coupling the (10 0) ten-proton states with the (14 0) fourteen-neutron states. The SU(3) irreps which label the coupled-basis states are (24 0), (22 1), (20 2), (18 3), (16 4), (14 5), (12 6), (10 7), (8 8), (6 9), (4 10). The Hamiltonian used for the calculations in the coupled system is again

$$\frac{H}{V_0} = -[(1-g)Q \cdot Q + g(S^\dagger S)], \tag{44}$$

where now

$$Q \cdot Q = Q_\pi \cdot Q_\pi + Q_\nu \cdot Q_\nu + 2Q_\pi \cdot Q_\nu \tag{45}$$

and

$$S^\dagger S = S_\pi^\dagger S_\pi + S_\nu^\dagger S_\nu + S_\pi^\dagger S_\nu + S_\nu^\dagger S_\pi. \tag{46}$$

The subscripts π and ν refer to the proton and neutron pieces of the operators, respectively. The $S_\pi^\dagger S_\nu$ and $S_\nu^\dagger S_\pi$ terms are not needed since we preserve both proton and neutron numbers.

A. Construction of the $Q \cdot Q$ and $S^\dagger S$ matrix elements

The angular momentum recoupling techniques used to derive the expressions for the matrix elements of the operators $Q_\pi \cdot Q_\nu$, $Q_\pi \cdot Q_\pi$, and $Q_\nu \cdot Q_\nu$ are similar to those outlined in Sec. V. The $Q_\pi \cdot Q_\nu$ matrix with initial and final states in the strongly coupled proton-neutron basis is written in terms of reduced matrix elements of the individual Q_π, Q_ν operators in their respective proton or neutron bases:

$$\begin{aligned}
&\langle[(\lambda'_\pi\mu'_\pi)I'_\pi \times (\lambda'_\nu\mu'_\nu)I'_\nu](\lambda'\mu')\rho'[K' \times I']J'M'|Q_\pi \cdot Q_\nu|[(\lambda_\pi\mu_\pi)I_\pi \times (\lambda_\nu\mu_\nu)I_\nu](\lambda\mu)\rho[K \times I]JM\rangle \\
&= \sum_{K_o I_o (\lambda_o\mu_o)\kappa_o \rho_{oo}\rho_\pi\rho_\nu\rho_o} \Big\{ \sqrt{5}\langle(\lambda'_\pi\mu'_\pi)I'_\pi \| Q^2_{I_p} \|(\lambda_\pi\mu_\pi)I_\pi\rangle_{\rho_\pi} \langle(10)1;(01)1||(\lambda_p\mu_p)K_p\rangle \\
&\times \langle(\lambda'_\nu\mu'_\nu)I'_\nu \| Q^2_{I_n} \|(\lambda_\nu\mu_\nu)I_\nu\rangle_{\rho_\nu} \langle(10)1;(01)1||(\lambda_n\mu_n)K_n\rangle \\
&\times \langle(\lambda_p\mu_p)K_p;(\lambda_n\mu_n)K_n||(\lambda_o\mu_o)K_o\kappa_o\rangle_{\rho_o} \langle(\lambda\mu)K\kappa;(\lambda_o\mu_o)K_o\kappa_o||(\lambda'\mu')K'\kappa'\rangle_{\rho_{oo}} \\
&\times \begin{bmatrix} (\lambda_\pi\mu_\pi) & (\lambda_\nu\mu_\nu) & (\lambda\mu) & \rho \\ (\lambda_p\mu_p) & (\lambda_n\mu_n) & (\lambda_o\mu_o) & \rho_o \\ (\lambda'_\pi\mu'_\pi) & (\lambda'_\nu\mu'_\nu) & (\lambda'\mu') & \rho' \\ \rho_\pi & \rho_\nu & \rho_{oo} & \end{bmatrix} \begin{bmatrix} I_\pi & I_\nu & I \\ I_p & I_n & I_o \\ I'_\pi & I'_\nu & I' \end{bmatrix} \begin{bmatrix} K & I & J \\ K_o & I_o & 0 \\ K' & I' & J \end{bmatrix} \begin{bmatrix} K_p & I_p & 2 \\ K_n & I_n & 2 \\ K_o & I_o & 0 \end{bmatrix} \Big\}.
\end{aligned} \tag{47}$$

The subscripts on the quantum numbers which label the proton and neutron basis states are π and ν respectively; for the proton and neutron operator the subscripts are p and n respectively; and for the coupled proton-neutron operator the subscript is o. The double-barred SU(3) $\supset$ SO(3) Wigner coefficients will require a band label, to be denoted by κ. This is included only in those symbols where it is needed. For the $(\lambda\mu) = (20\ 2)$ irrep, for example, the two states with angular momentum $K = 2$ are distinguished by the two possible values of κ. We use the prolate prescription for the label κ in the Draayer-Akiyama code [12] when $\lambda \geq \mu$. The multiplicity in the coupling of the the SU(3) irrep $(\lambda\mu)$ for the initial proton-neutron basis state and the SU(3) irrep $(\lambda_o\mu_o)$ for the proton-neutron operator to give the SU(3) irrep $(\lambda'\mu')$ for the final proton-neutron basis state is ρ_{oo}. The special case of interest has generalized seniority quantum numbers $u = u' = 0$. This implies that the total I-spins such as $I'_\pi = I_\pi = I'_\nu = I_\nu = 0$. In addition, by choosing $(\lambda'_\pi\mu'_\pi) = (\lambda_\pi\mu_\pi) = (10\ 0)$, and $(\lambda'_\nu\mu'_\nu) = (\lambda_\nu\mu_\nu) = (14\ 0)$, we eliminate the need for the multiplicity labels $\rho, \rho', \rho_0, \rho_\pi, \rho_\nu$ and also simplify the $9j$,$9(\lambda\mu)$ and SU(3)-Wigner coefficients. The symmetry of these coefficients further restricts the quantum numbers to : $I = I' = I_p = I_n = I_o = 0$, hence $K_o = 0$; $K_p = K_n = 2$; and $K = K' = J = J'$. This now limits the values of $(\lambda_p\mu_p)$ and $(\lambda_n\mu_n)$ both to (11) and eliminates the need for the label κ_o. There are two terms in the sum with $(\lambda_o\mu_o) = (22)$ and (00). The final sum includes the multiplicity quantum number ρ_{oo}. The expression which results is given below for the $Q_\pi \cdot Q_\nu$ matrix:

$$\begin{aligned}
&\langle[(10\ 0)0 \times (14\ 0)0](\lambda'\mu')K'M'|Q_\pi \cdot Q_\nu|[((10\ 0)0 \times (14\ 0)0](\lambda\mu)KM\rangle \\
&= \sum_{(\lambda_o\mu_o)\rho_{oo}} \Big\{ \sqrt{5}\langle(10\ 0)I'_\pi = 0 \| Q_{\pi I_p=0} \|(10\ 0)I_\pi = 0\rangle \langle(10)1;(01)1||(11)2\rangle \\
&\times \langle(14\ 0)I'_\nu = 0 \| Q_{\nu I_n=0} \|(14\ 0)I_\nu = 0\rangle \langle(10)1;(01)1||(11)2\rangle \\
&\times \langle(11)2;(11)2||(\lambda_o\mu_o)0\rangle \langle(\lambda\mu)K\kappa;(\lambda_o\mu_o)0||(\lambda'\mu')K'\kappa'\rangle_{\rho_{oo}} \begin{bmatrix} (10\ 0) & (14\ 0) & (\lambda\mu) \\ (11) & (11) & (\lambda_o\mu_o) \\ (10\ 0) & (14\ 0) & (\lambda'\mu') \\ - & - & \rho_{oo} \end{bmatrix} \Big\}.
\end{aligned} \tag{48}$$

The analytical form for the $Q_\pi \cdot Q_\pi$ matrix used in our calculation is given by

$$\begin{aligned}
&\langle[(10\ 0)0 \times (14\ 0)0](\lambda'\mu')K'M'|Q_\pi \cdot Q_\pi|[((10\ 0)0 \times (14\ 0)0](\lambda\mu)KM\rangle \\
&= \sum_{K_\pi=0}^{10} \sum_{K_\nu=0}^{14} \{\langle(10\ 0)K_\pi = J_\pi I_\pi = 0||Q_\pi \cdot Q_\pi||(10\ 0)K_\pi = J_\pi I_\pi = 0\rangle \delta_{\nu\nu'} \langle(10\ 0)K_\pi;(14\ 0)K_\nu||(\lambda'\mu')K'\kappa'\rangle \\
&\times \langle(10\ 0)K_\pi;(14\ 0)K_\nu||(\lambda\mu)K\kappa\rangle\}
\end{aligned} \tag{49}$$

with only even values for K_π and K_ν. The expressions for the matrix elements of $Q_\nu \cdot Q_\nu$, $S_\pi^\dagger S_\pi$, and $S_\nu^\dagger S_\nu$ can be obtained from Eq. (49) by replacing the operators in the double-barred matrix element, the quantum numbers, and the values of K_π and K_ν with the appropriate ones.

B. Results

In Fig. 5 we present the percentage of the dominant basis states in the three lowest eigenstates of $J = 0$ as a function of $1 - g$ for the 24 particle system. Recall that there are two independent phase choices for the coefficients of Q_μ^2 for the protons and four for the neutrons. The calculations were performed for all the eight possible combinations for the coupled system, but the results are shown for only four of them in Fig. 5. As before, the values of $1 - g$ range from 0.0 to 1.0 in increments of 0.2. We shall also focus on the value of $1 - g = 0.12$ which is the average of the values of $1 - g$ for the protons and neutrons of actinide nuclei extracted from the work of Kumar and Baranger.

Since $J = 0$ occurs only in irreps with λ and μ both even, the six basis states which comprise the $J = 0$ eigenstates are restricted to the SU(3) irreps (24 0), (20 2), (16 4), (12 6), (8 8), and (4 10). If the FDSM-SU(3) symmetry is to show Elliott-type SU(3) characteristics, then we would expect the eigenstates to appear in the same order. This implies that the dominant contribution to the lowest $J = 0$ eigenstate should be from the state with (24 0). The second lowest $J = 0$ eigenstate should be predominantly (20 2) and the third lowest $J = 0$ eigenstate should be predominantly (16 4). It is clear from Fig. 5 that this pattern emerges only for the phase combination labeled (a). The calculation for this case uses the coefficients of Q_μ^2 labeled phase 2 for both the protons and the neutrons. The contribution of the basis states with (24 0) is greater than 99% for values of $1 - g > 0.2$, of those with (20 2) for $1 - g > 0.4$, and of those with (16 4) for $1 - g > 0.6$. The phase combination labeled (b) is the worst of the four since, for all three eigenstates, the dominant contribution does not come from the expected basis states. For the phase combination (c) the state with (20 2) is the dominant component of the second lowest eigenstate but only for values of $1 - g$ between 0.0 and 0.3. The result for the phase combination (d) is better than for (c), with the state (24 0) being the dominant component of the lowest eigenstate for all values of $1 - g$.

This vast discrepancy in the results for the different phase combinations is difficult to understand in the context of the the results of Sec. VI where we saw that the coefficients of the basis states with (10 0) for the protons and (14 0) for the neutrons were practically zero regardless of the phase choice. However, a possible source of the discrepancy is identified by considering the $Q_\pi \cdot Q_\nu$, $Q_\pi \cdot Q_\pi$, and $Q_\nu \cdot Q_\nu$ terms in the effective interaction which are sensitive to the phase choices.

By restricting the basis to include only the (10 0) proton and (14 0) neutron states, we have minimized the size of the double-barred matrix elements in Eq. (49) considerably and have reduced the phase-dependent influence of the $Q_\pi \cdot Q_\pi$ and $Q_\nu \cdot Q_\nu$ terms. The ordering of the $(\lambda\mu)$ states is thus largely dependent on the SU(3)-Wigner coefficients of Eq. (48) and is also affected by the sign and magnitude of the triple-barred matrix elements of Q_π and Q_ν. Moreover, in the pure (10 0) and (14 0) states, these diagonal matrix elements now gain contributions only from two terms, namely, those with coefficients $C_{ii'K_p=2I_p=0}$ with $i = i' = \frac{1}{2}$ and $i = i' = \frac{7}{2}$ for Q_π and $i = i' = \frac{3}{2}$ and $i = i' = \frac{9}{2}$ for Q_ν as seen from Eq. (26). Operators with $I_p \neq 0$ make no contribution because of the severe basis truncation. We tabulate the product of the two diagonal-triple-barred matrix elements for all the possible phase combinations in Table IX.

The value of the product for the phase combination labeled (a) in Fig. 5 or phase 2 and phase 2 in Table IX is the most positive whereas that for (b) in Fig. 5 or phase 2 and phase 1 in Table IX is the most negative. This corresponds to the results discussed above where the ordering of the SU(3) irreps is closest to the Elliott ordering for (a) and farthest for (b). Recall from Sec. IV that the phase

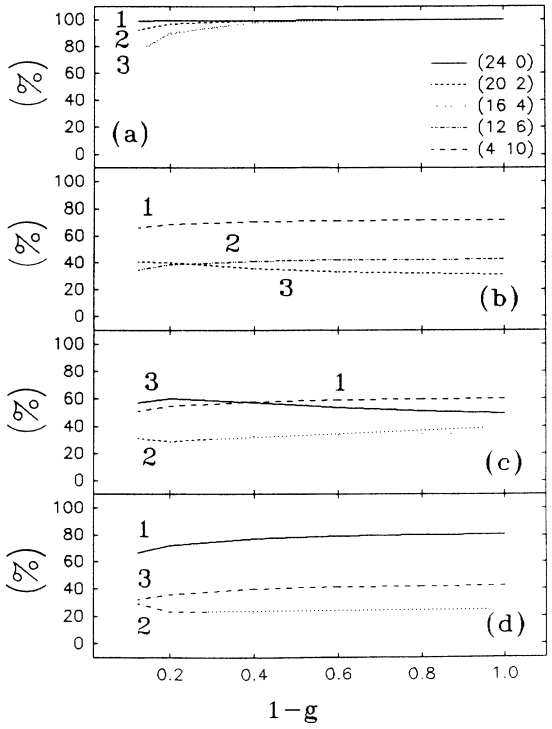

FIG. 5. The percentage of the dominant basis states in the three lowest eigenstates (1,2,3) of $J = 0$ for the coupled basis using four possible phase combinations: (a) phase 2 for the $N = 5$ shell and phase 2 for the $N = 6$ shell, (b) phase 2 for the $N = 5$ shell and phase 1 for the $N = 6$ shell, (c) phase 1 for the $N = 5$ shell and phase 2 for the $N = 6$ shell, (d) phase 1 for the $N = 5$ shell and phase 1 for the $N = 6$ shell. In the plot labeled 2 in (c) and (d), the dominant basis state labeled with the SU(3) irrep (20 2) and (4 10) respectively, changes to one with (16 4). The lines are joined as would be expected if the points at the transition area had been calculated explicitly.

TABLE IX. The product of the two diagonal-triple-barred matrix elements of $Q_{\pi o}$ and $Q_{\nu o}$.

Phase 1 Phase 1	Phase 1 Phase 2	Phase 2 Phase 1	Phase 2 Phase 2	Phase 1 Phase 4	Phase 1 Phase 6	Phase 2 Phase 4	Phase 2 Phase 6
+ 8.6	− 11.9	− 56.1	+ 77.5	− 3.4	+ 0.11	+ 22.1	− 0.69

combination (a) has the same type of phase convention for both protons and neutrons, all radial functions being positive in the limit of r going to 0. The higher value of the product for (d) compared to (c) is also in keeping with the earlier discussion for these phase combinations. The plots for the other phase combinations are not shown here but the percentages of the dominant basis states have been calculated. We found that the correspondence between the values of the products of the triple-barred matrix elements of Q_π and Q_ν in Table IX, and the ordering of the SU(3) irreps in the strong-coupling limit holds for these cases also. We conclude that the FDSM-SU(3) symmetry shows Elliott-type characteristics if the contribution of the $Q_\pi \cdot Q_\nu$ term with an attractive coupling strength in the Hamiltonian of Eq. (44) is the largest. This is in keeping with standard nuclear structure calculations which indicate a connection between large coupling strengths for the $Q_\pi \cdot Q_\nu$ term and rotational bands. However, the issue of a muliplicity of FDSM bases needs to be addressed by the founders of the FDSM to explain why only one of the eight possible combinations works so well.

As a final analysis of the SU(3) symmetry in the coupled basis in the k-active scheme of the FDSM, we present an energy level diagram in Fig. 6 for the favored phase combination (a) with $1 - g = 0.12$. The rotational bands shown are ordered according to the SU(3) irreps (24 0), (22 1), (20 2), (18 3) and (16 4). There are seemingly two bands for the state with (22 1). This is because the odd values of J beginning with $J = 1$ have been separated from the even values of J beginning with $J = 2$ and have been placed into two separate columns due to a relatively large odd-J and even-J staggering of the energy levels of this single "K_J" = 1 band. This staggering also results in seemingly three bands with minimum J values of ($J_{\min} = 0, 2, 3$) for the state with (20 2) instead of two "K_J" bands, with "K_J" = 0 and 2, four ($J_{\min} = 1, 2, 3, 4$) for the state with (18 3) instead of two, and five ($J_{\min} = 0, 2, 3, 4, 5$) for the state with (16 4) instead of three. We also show the bandheads for $J_{\min} = 0$ or $J_{\min} = 1$ for the states with the irreps (14 5), (12 6), (10 7), (8 8), (6 9), and (4 10). The percentages of the basis states labeled with the expected SU(3) irreps for a particular eigenstate are very high for the lower bands and decrease for the higher bands. In Fig. 7, we show the rotational nature of the bands shown in Fig. 6 by plotting the energy as a function of $J(J + 1)$. The number of bands in Fig. 7 are also accounted for by the even-J and odd-J staggering of the bands with $K_J \neq 0$. In the ideal case, for a perfect rotational band, we should get a straight line as seen for the single band for (24 0). From the plots in Fig. 7 we conclude that the bands are indeed quite rotational.

These results show that the SU(3) eigenstates in a strongly coupled FDSM basis with the favored phase combination are rotational provided that the necessary renormalization has been performed in the separate proton and neutron basis to ensure that the states with (10 0) and (14 0) are the dominant components of the lowest eigenstates.

VIII. SUMMARY AND CONCLUSIONS

In this paper we have studied the fundamental assumptions made in the fermion dynamical symmetry model (FDSM). In the FDSM, it is assumed that the lowest

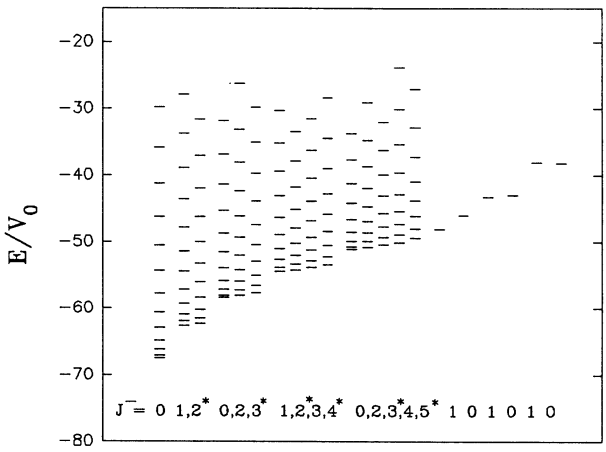

FIG. 6. Rotational bands for states with predominant SU(3) symmetry (24 0), (22 1), (20 2), (18 3), and (16 4), along with $J = 0$ or $J = 1$ bandheads for states with predominant SU(3) symmetry (14 5), (12 6), (10 7), (8 8), (6 9) and (4 10) . The bandhead J values are designated by J^-. These spectra are calculated for phase 2 in the $N = 5$ and $N = 6$ shells with $1 - g = 0.12$. The energy levels in the band whose J value for the bandhead is denoted by an asterisk and those in the band immediately to its left belong to the same "K_J" branch of a rotational band. The energy levels with even and odd J values are shown in separate adjacent columns since there is considerable even-odd staggering within a band. For example, the two columns designated $J^- = 1, 2^*$ are the staggered odd and even J members of the (22 1) band with a single "K_J" = 1 branch, the two columns designated $J^- = 2, 3^*$ are the staggered even and odd J members of the "K_J" = 2 branch of (20 2) while $J^- = 0$ gives its "K_J" = 0 branch of even J values only, and so on. The "K_J" notation is chosen to correspond to the conventional nuclear K-branch notation. In the text "K_J" occurs in the SU(3) ⊃ SO(3) Wigner coefficients, where it is replaced by κ.

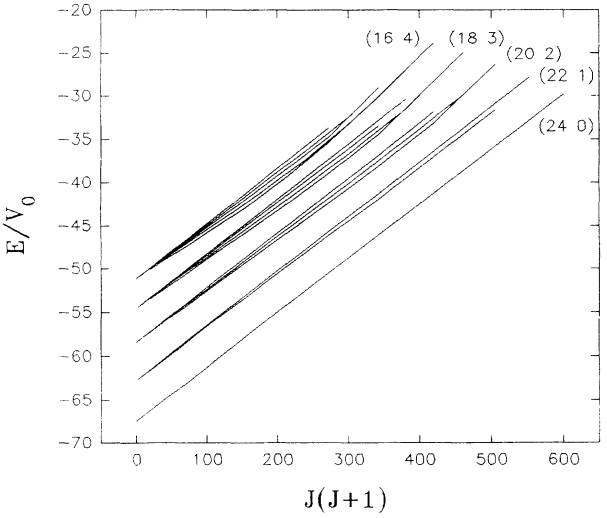

FIG. 7. Rotational nature of the bands. The larger number of lines plotted for each SU(3) irrep reflects the even-J and odd-J staggering in the bands shown in Fig. 6.

eigenstates of even nuclei are dominated by states built from the favored S and D pairs only, i.e., by states with generalized seniority $u = 0$. In the Sp(6) $\supset$ U(3) branch of the model, moreover, it is assumed that the lowest eigenstates of actinide nuclei are states with the largest SU(3) quantum numbers permitted in the model. The FDSM basis space built on these two assumptions is the type of severe truncation of the shell model space needed in order to perform calculations in heavy deformed nuclei such as the actinides. To assess the validity of such a severe truncation let us consider the overlap between a symmetry dictated model space like that of the FDSM with the lowest eigenstates of the full shell model space. If U is the unitary transformation which transforms the basis states of the model space, $|\psi_m\rangle$, to the corresponding lowest states of the shell model space, $|\psi_s\rangle$, and the model Hamiltonian H_m is related to the shell model effective Hamiltonian H_s by $H_m = UH_sU^\dagger$, then

$$\begin{aligned}\langle\psi_s|H_s|\psi_s\rangle &= \langle\psi_s U^\dagger\,|U\ H_s\ U^\dagger\ |U\psi_s\rangle \\ &= \langle\psi_m\ |H_m|\psi_m\rangle. \end{aligned} \tag{50}$$

If the overlaps

$$\langle\psi_s|\psi_m\rangle = \langle\psi_s|U\psi_s\rangle \tag{51}$$

are close to unity, then the eigenstates of the model, such as the FDSM, would be close to the lowest eigenstates of the shell model and the shell model effective interactions could be mapped into the model space by perturbative methods. On the other hand, if the overlaps are close to zero, it would be virtually impossible to calculate U, and the mapping from the shell model space to the model space becomes extremely complicated. With this perspective in mind, the results obtained from the calculations which were performed for systems of protons and neutrons filling the valence shells appropriate for the actinide region can be summarised as follows.

A semirealistic effective interaction consisting of an FDSM pairing plus a quadrupole-quadrupole term was diagonalized in a complete two-particle basis which was expanded in terms of states with $u = 0$ and $u = 2$. The results for the lowest $J = 0, 2$ eigenstates were analyzed. The percentage of the state with $u = 0$ was small, particularly in the lowest $J = 2$ eigenstates, and decreased as the strength of the $Q \cdot Q$ term was increased. This implies that the FDSM basis states have a small overlap with the lowest $J = 2$ shell model eigenstates.

As a next test of the FDSM assumptions, a single $J = 0$ pairing plus quadrupole-quadrupole interaction was diagonalized in the $u = 0$ subspace separately for (i) ten protons in the $N = 5$ shell and (ii) fourteen neutrons in the $N = 6$ shell. These identical particle systems were chosen for two reasons. First, they contain the largest possible FDSM-SU(3) quantum numbers for the actinide region, namely, (10 0) for the protons and (14 0) for the neutrons, thereby having the largest potential for collectivity. Secondly, these systems contain a fairly rich configuration of both large and small SU(3) quantum numbers. For both the pure proton and the pure neutron calculations the eigenstates did not exhibit the ordering expected of an SU(3) rotational symmetry. The states with (10 0) contribute less than 0.3% to the lowest eigenstates in the ten-proton calculation for all values of the coupling strength of $Q \cdot Q$. Similarly, for the fourteen-neutron calculation, the (14 0) contribution to the lowest eigenstates is very close to zero. Again, the overlap between the lowest eigenstates and the expected FDSM-SU(3) basis states is close to zero. Due to the smallness of the overlaps even with our simple effective shell model interaction of the Kumar-Baranger type, the plans to use more realistic Kuo-Brown interactions were abandoned, since we would not expect a qualitative change in this basic result.

An important result of this study is the discovery that there is more than one FDSM basis. This multiplicity of FDSM bases arises because the overlaps between the shell model basis and the FDSM basis depend on the choice of the relative signs of the harmonic oscillator radial wave functions with different values of the orbital angular momentum quantum number l. There are two independent FDSM bases for the $N = 5$ shell and four for the $N = 6$ shell. This fact was not apparent in the original formulation of the FDSM, since the transformation of the group generators from the shell model $j - j$ basis to the FDSM $k - i$ basis does not include the radial functions. It does become apparent at once when the real quadrupole moment operator is transformed to the $k - i$ basis. Results for physical quantities such as energy eigenvalues cannot be dependent on such phase choices when calculations are carried out in a full shell model basis, as verified by the complete two-particle calculations. However, the results in a truncated FDSM basis are very sensitive to these phase choices as illustrated dramatically by our final calculation for a coupled-proton-neutron system.

In this calculation we attempt to answer the following question. Does an effective interaction with a strong

$Q_\pi \cdot Q_\nu$ component drive the coupled-proton-neutron system into the most collective SU(3) representations with well-established rotational structure? Despite the results for the separate ten-proton and fourteen-neutron systems where the states with the SU(3) irreps (10 0) and (14 0) are extremely minor components of the lowest eigenstates, we force them to be the dominant components of the lowest eigenstates for the coupled-24-nucleon system. Of the eight possible FDSM bases corresponding to the $2 \times 4 = 8$ possible phase combinations for this system, only one led to the expected pattern of SU(3) irreps for a rotational nucleus. For this phase choice, rotational bands are predicted when a $J = 0$ pairing plus quadrupole-quadrupole interaction of the Kumar-Baranger type is diagonalized in the strongly coupled-proton-neutron basis. Moreover, the ground state band is a nearly pure (24 0) band; the first excited band with a staggered even-J and odd-J structure is predominantly a (22 1) band; followed in order by bands which are dominated by the expected SU(3) symmetries (20 2), (18 3), and (16 4). The phase choice for the various possible FDSM bases which leads to these excellent SU(3) characteristics of the type expected for rotational nuclei is the one for which the contribution of the $Q_\pi \cdot Q_\nu$ term to the matrix elements of the effective interaction is by far the largest.

The fermion pair structure in the FDSM basis which leads to the dynamical symmetry in the Hamiltonians is indeed a mathematically convenient one for the purposes of model building in a workable algebraic framework. The original purpose of Ginocchio's fermion pair algebra was to better understand the boson space of the IBM and to simplify the mapping from the shell model fermion space to the less complicated boson space. It should be remembered that the S and D pairs of the fermion pair algebra are identical nucleon pairs, i.e., pure proton pairs or pure neutron pairs. It is thus disappointing that the overlaps between the truncated FDSM basis states and the lowest shell model eigenstates are so small in pure proton or pure neutron configurations. Our 24-nucleon calculation perhaps gives some indication of how the Sp(6) ⊃ U(3) truncation scheme of the FDSM may be salvaged in the actinide region. With a choice of the proper FDSM basis, a strong attractive $Q_\pi \cdot Q_\nu$ interaction may possibly single out those pure proton and pure neutron SU(3) irreps which are only a tiny fraction of the shell model eigenstates in the pure proton or pure neutron configurations. If these are the grounds for the validity of the FDSM, then we have to conclude that the mapping from the shell model fermion space to the FDSM fermion space is just as complicated as the mapping to the IBM boson space. The advantage of having fermion pairs as the basic building blocks of the model is partially lost.

The group-theoretical methods pioneered by Elliott have stimulated a continuing interest in algebraic models using symmetry groups as a guide for making approximations in many-nucleon systems with strong collective properties. By probing the assumptions made in one of these models, the FDSM, we have arrived at somewhat contradictory conclusions. One hopes that this work will lead to a more careful evaluation of the limitations of the FDSM as a nuclear model based on fermion S and D pairs.

ACKNOWLEDGMENTS

One of us (S.R.S) would like to thank C. A. Orme and F. J. Lamelas for help in making the figures, and the staff of the Missouri University Research Reactor for their hospitality during the preparation of this manuscript. This work was supported by the U.S. National Science Foundation.

[1] J. P. Elliott, Proc. R. Soc. London Ser. A **245**, 128 (1958); A **245**, 562 (1958).
[2] J. P. Elliott and M. Harvey, Proc. R. Soc. London Ser. A **272**, 55 (1963).
[3] R. D. Ratna Raju, J. P. Draayer, and K. T. Hecht, Nucl. Phys. **A202**, 433 (1973).
[4] D. Braunschweig and K. T. Hecht, Phys. Lett. **77B**, 33 (1978).
[5] A. Arima and F. Iachello, Ann Phys. (N.Y.) **99**, 253 (1976).
[6] J. N. Ginocchio, Ann. Phys. **126**, 234 (1980).
[7] C. L. Wu, D. H. Feng, X. G. Chen, J. Q. Chen, and M. W. Guidry, Phys. Lett. **168B**, 313 (1986); Phys. Rev. C **36**, 1157 (1987); J. Q. Chen, D. H. Feng, and C. L. Wu, *ibid.* C **34**, 2269 (1986).
[8] P. Halse, Phys. Rev. C **36**, 372 (1987).
[9] P. Halse, Phys. Rev. C **39**, 1104 (1989).
[10] J. Q. Chen, D. H. Feng, M. W. Guidry, and C. L. Wu, Phys. Rev. C **44**, 559 (1991).
[11] P. Halse, Phys. Rev. C **44**, 562 (1991).
[12] J. P. Draayer and Y. Akiyama, J. Math. Phys. **14**, 1904 (1973); Comput. Phys. Comm. **5**, 405 (1973).
[13] H. Ower *et al.*, Nucl. Phys. **A388**, 421 (1982).
[14] K. T. Hecht, Nucl. Phys. **A484** 61 (1988).
[15] Sudha R. Swaminathan, Ph.D. thesis, University of Michigan, 1993 (unpublished).
[16] K. T. Hecht and J. Q. Chen, Nucl. Phys. **A512**, 365 (1990).
[17] K. T. Hecht, *The Vector Coherent State Method and Its Application to Problems of Higher Symmetries*, Lecture Notes in Physics Vol. 290 (Springer, Berlin, 1987).
[18] J. P. Draayer and Y. Leschber, *Branching Rules for Unitary Symmetries of the Nuclear Shell Model* (Lousiana State University, Baton Rouge, 1987).
[19] K. Kumar and M. Baranger, Nucl. Phys. **A62**, 113 (1965); **A110**, 490 (1968); **A110**, 529 (1968); **A122**, 241 (1968); **A122**, 273 (1968).